Portland State University
PDXScholar

Civil and Environmental Engineering Faculty Publications and Presentations

Civil and Environmental Engineering

9-2012

Value of Travel Time Reliability Part II: A Study of Tradeoffs Between Travel Reliability, Congestion Mitigation Strategies and Emissions

Miguel A. Figliozzi
Portland State University, figliozzi@pdx.edu

Alexander Y. Bigazzi
Portland State University, abigazzi@gmail.com

Let us know how access to this document benefits you.

Follow this and additional works at: http://pdxscholar.library.pdx.edu/cengin_fac

Part of the Civil and Environmental Engineering Commons, and the Transportation Commons

Citation Details

Figliozzi, M. and Bigazzi, A. Value of Travel Time Reliability Part II: A Study of Tradeoffs Between Travel Reliability, Congestion Mitigation Strategies and Emissions. OTREC-RR-11-12B. Portland, OR: Transportation Research and Education Center (TREC), 2012.

This Report is brought to you for free and open access. It has been accepted for inclusion in Civil and Environmental Engineering Faculty Publications and Presentations by an authorized administrator of PDXScholar. For more information, please contact pdxscholar@pdx.edu.

OTREC

OREGON TRANSPORTATION RESEARCH AND EDUCATION CONSORTIUM

FINAL REPORT

Value of Travel Time Reliability Part II: A study of Tradeoffs Between Travel Reliability, Congestion Mitigation Strategies and Emissions

OTREC-RR-11-12B
September 2012

A National University Transportation Center sponsored by the U.S. Department of Transportation's Research and Innovative Technology Administration

VALUE OF TRAVEL-TIME RELIABILITY PART II: A STUDY OF TRADEOFFS BETWEEN TRAVEL RELIABILITY, CONGESTION-MITIGATION STRATEGIES AND EMISSIONS

Final Report

OTREC-RR-11-12B

by

Miguel Figliozzi, Ph.D.
Alex Bigazzi

Portland State University

for

OTREC
OREGON TRANSPORTATION RESEARCH AND EDUCATION CONSORTIUM

P.O. Box 751
Portland, OR 97207

September 2012

Technical Report Documentation Page

1. Report No. OTREC-RR-11-12B	2. Government Accession No.	3. Recipient's Catalog No.
4. Title and Subtitle		5. Report Date September 2012 6. Performing Organization Code
7. Author(s) Miguel Figliozzi Alex Bigazzi		8. Performing Organization Report No.
9. Performing Organization Name and Address Portland State University Civil and Environmental Engineering P.O. Box 751 Portland, OR, 97207		10. Work Unit No. (TRAIS) 11. Contract or Grant No. 2009-248
12. Sponsoring Agency Name and Address Oregon Transportation Research and Education Consortium (OTREC) P.O. Box 751 Portland, Oregon 97207		13. Type of Report and Period Covered 14. Sponsoring Agency Code
15. Supplementary Notes		

16. Abstract

Capacity, demand, and vehicle based emissions reduction strategies are compared for several pollutants employing aggregate US congestion and vehicle fleet condition data. We find that congestion mitigation does not inevitably lead to reduced emissions; the net effect of mitigation depends on the balance of induced travel demand and increased vehicle efficiency that in turn depend on the pollutant, congestion level, and fleet composition. In the long run, capacity-based congestion improvements within certain speed intervals can reasonably be expected to increase emissions of CO2e, CO, and NOx through increased vehicle travel volume. Better opportunities for emissions reductions exist for HC and PM2.5 emissions, and on more heavily congested arterials. Advanced-efficiency vehicles with emissions rates that are less sensitive to congestion than conventional vehicles generate less emissions co-benefits from congestion mitigation.

17. Key Words Congestion mitigation, Emissions reductions, Vehicle emissions, Traffic management	18. Distribution Statement No restrictions. Copies available from OTREC: www.otrec.us

19. Security Classification (of this report) Unclassified	20. Security Classification (of this page) Unclassified	21. No. of Pages 66	22. Price

ACKNOWLEDGEMENTS

The authors gratefully acknowledge the Oregon Transportation Research and Education Consortium (OTREC) for sponsoring this project. Any errors or omissions are the sole responsibility of the authors.

DISCLAIMER

The contents of this report reflect the views of the authors, who are solely responsible for the facts and the accuracy of the material and information presented herein. This document is disseminated under the sponsorship of the U.S. Department of Transportation University Transportation Centers Program in the interest of information exchange. The U.S. Government assumes no liability for the contents or use thereof. The contents do not necessarily reflect the official views of the U.S. Government. This report does not constitute a standard, specification or regulation.

TABLE OF CONTENTS

LIST OF TABLES

LIST OF FIGURES

EXECUTIVE SUMMARY

There is a growing concern about the costs of congestion on urban mobility, urban air quality, and greenhouse gas emissions. The full effects of traffic congestion on motor-vehicle emissions are still not well quantified because of interactions and impacts on many scales, from vehicle maintenance to land use. This research provides a new understanding of the tradeoffs between travel-time reliability, congestion mitigation and emissions. We develop a model to study the impacts of travel-time reliability costs in terms of delays, fuel and emissions costs. We apply our model to: (a) a congested freeway corridor in Portland, OR. and (b) six distinct urban areas in the U.S. In the freeway case, results clearly indicate that travel time is the dominant cost, followed by fuel costs. For a given value per trip (in dollars/mile), the traffic-flow volume that maximizes social benefits decreases as travel-time reliability decreases. Comparing six distinct U.S. urban areas, of varying size and density, using macroscopic peak-period traffic characteristics we see that the impact of travel-time reliability is significant for larger and denser urban areas.

This research also analyzes capacity-, demand- and efficiency-based emissions-reduction strategies. A novel, parsimonious, methodological framework is developed to estimate these strategies on different pollutants. Several interesting results are found by employing aggregate data representing U.S. congestion and vehicle-fleet conditions to estimate emissions changes for greenhouse gases (CO2e), carbon monoxide (CO), nitrogen oxides (NOx), fine particulate matter (PM2.5), and hydrocarbons (HC). First, congestion mitigation does not inevitably lead to reduced emissions. The net effect of congestion mitigation depends on the balance of induced travel demand and increased vehicle efficiency – which, in turn, depend on the pollutant, congestion level and fleet composition. In general, capacity-based congestion improvements within certain speed intervals (e.g., 30 to 40 mph) can reasonably be expected to increase total emissions of CO2e, CO and NOx in the long run through increased vehicle-travel volume. Better opportunities for emissions reductions exist for HC and PM2.5 emissions, and on more heavily congested arterials. Efficiency- and demand-based reduction strategies provide attractive alternatives to capacity-based strategies. Still, reducing light-duty vehicle emissions alone has only a limited impact – especially on PM2.5 emissions. Advanced-efficiency vehicles with emissions rates that are less sensitive to congestion than conventional vehicles generate less emissions co-benefits from congestion mitigation.

In conclusion, reducing travel-time variability is essential to reduce unnecessary delays, fuel costs and emissions. However, increasing travel speeds (e.g., from 30 to 40 mph) can lead to higher total emissions because there are complex interactions between travel demand, fleet composition,and pollutant type.

1.0 INTRODUCTION

1.1 BACKGROUND

There is a growing concern about the costs of congestion on urban mobility, urban air quality, and greenhouse gas emissions. The full effects of traffic congestion on motor-vehicle emissions are still not well quantified because of interactions and impacts on many scales, from vehicle maintenance to land use. This research provides a new understanding of the tradeoffs between travel-time reliability, congestion mitigation and emissions.

Traffic congestion impacts urban areas throughout the world with varying economic, social and environmental costs. Policymakers, researchers and activists often assume that unreliability and congestion reductions inevitably lead to reduced vehicle emissions. In many cases, emissions reductions are cited as an implicit benefit of congestion mitigation without proper justification or quantification of the benefits. For example, the U.S. Federal Highway Administration's Congestion Mitigation and Air Quality (CMAQ) Improvement Program suggests a clear co-beneficial relationship between the two. Excess travel time is consistently the largest estimated social cost of congestion, but comprehensive attempts to quantify total congestion impacts suffer from challenges such as estimating the extent of higher-order, indirect effects (e.g., congestion impacts on land use) and quantifying intangibles (e.g., traveler stress levels). Too often, congestion cost analyses do not even go as far as to estimate driver-behavior responses to congestion (such as mode shift).

1.2 RESEARCH GOALS AND REPORT ORGANIZATION

This research tackles the problem of congestion, travel-time reliability and emissions tradeoffs. Several questions are answered:

(1) What are the relative short-term impacts of travel-time reliability on travel time, fuel and greenhouse gas emissions? What are the impacts of travel-time reliability across different cities, in terms of total travel demand and density, in the U.S.?

(2) What are the long-term impacts of strategies that aim to reduce congestion (i.e., increase travel speed)? Are travel speed increases always beneficial across different fleet compositions and emission types?

Section 2.0 presents a methodology to study the short-term costs of freeway travel-time unreliability in terms of delays, fuel and emissions costs. This methodology is applied in Section 3.0 to study (a) a congested freeway corridor in Portland, OR., and (b) six distinct urban areas in the U.S. Section 4.0 discusses potential long-term impacts of congestion-reduction strategies and different strategies that can be applied either in terms of capacity changes, vehicle-technology changes, or using demand-management strategies. A methodology to study the long-term impacts of congestion-reduction strategies on emissions is developed in Section 5.0. Sections 6.0, 7.0 and 8.0 discuss the impacts of capacity, vehicle technology and demand-based strategies,

respectively. Section 10.0 discusses the impacts of fleet composition (i.e., percentage of passenger vehicles and heavy-duty vehicles) on total emissions. Section 11.0 ends with conclusions.

2.0 METHODOLOGY TO STUDY THE IMPACT OF RELIABILITY ON COSTS

Traffic congestion is increasing around the world, particularly on urban freeways (European Conference of Ministers of Transport (ECMT), 2007; Schrank and Lomax, 2009). Congestion has enormous social and financial impacts related to travel time, air pollution, fuel consumption, freight costs and safety costs, among others (Goodwin, 2004; HDR, 2009; Kriger et al., 2007; Weisbrod, Vary and Treyz, 2001). In terms of travel time and freight costs, we also now appreciate that it is not only average conditions, but unreliable/variable conditions that increase total costs of congestion (Brownstone and Small, 2005; Danielis, Marcucci and Rotaris, 2005).

One of the causes of unreliability is instability in a traffic stream as it nears some maximal throughput capacity (Kerner, 1999; May, 1989). Minor disturbances or perturbations can cause unstable traffic streams to break down into queued or bottleneck conditions, with the accompanying heavy-congestion costs. But the traffic volume at which flow breaks down is not a certainty, motivating past research to model networks as having uncertain traffic-volume capacity (Boyles, Kockelman and Travis Waller, 2010; Lam, Shao and Sumalee, 2008; Lo, Luo and Siu, 2006; Chen et al., 2002). Lo and Tung (2003) modeled link capacities as uniformly distributed random variables, while Brilon (2005) modeled traffic capacity as a stochastic variable following a Weibull distribution. Since traffic-flow breakdown is a stochastic event, it should also be treated as such in traffic management. In an effort to better utilize existing roadway capacity, many metropolitan areas have established advanced traffic management systems (ATMS). These systems employ various traffic-control techniques such as ramp metering, variable speed limits, dynamic congestion pricing, and dynamic traveler guidance (U.S. Department of Transportation, n.d.).

The proliferation of ATMS provides opportunities to better manage traffic flows. We propose that traffic flows can be better managed if the impacts of stochastic freeway capacity on delays, fuel consumption and emissions are properly modeled. We apply a stochastic freeway-capacity model of traffic-flow social benefits and costs to a congested freeway corridor in Portland using archived traffic data. Finally, we make comparisons across a diverse set of urban areas to illustrate relationships between urban density, trip length and congestion levels.

We contrast the models that result from assuming (a) constant freeway capacity (reliable travel times) and (b) a stochastic freeway-capacity model (unreliable travel times).

2.1 CONSTANT FREEWAY CAPACITY

Notation.

λ: traffic demand or vehicle arrival rate [vehicles/hour]

λ_c: roadway capacity [vehicles/hour]

$t(\lambda)$: travel rate, time to travel one mile with demand rate λ [hour/mile]

$v(\lambda) = 1/t(\lambda)$: average travel speed [miles/hour]

$e(\lambda)$: marginal emissions rate, with demand rate λ [kg/veh-mile]

$f(\lambda)$: fuel consumption rate, with demand rate λ [gallons/veh-mile]

l: length of the freeway section under study [miles]

c_e: cost of emissions (of pollutant in $e(\lambda)$) [$/kg]

c_t: value of time [$/hour]

c_f: cost of fuel [$/gallon]

Travel Rate. Using the well-known Bureau of Public Roads (BPR) volume/travel-time function (1964), the travel rate as a function of arrival rate λ (assumed constant over the analysis period) is:

$$\boldsymbol{t(\lambda) = t_o\left(1 + a\left(\lambda/\lambda_c\right)^b\right) = t_o + t_o a\left(\lambda/\lambda_c\right)^b} \quad (1)$$

where t_o is the free-flow travel rate and a and b are parameters.

Emissions and Fuel Rates. For emissions we estimate a function of λ *per vehicle, per mile*, $e(\lambda)$. The CO_2 emissions estimates used for fitting in this study are from Bigazzi and Figliozzi (2011) and are based on the **Mo**tor **V**ehicle **E**missions **S**imulator (MOVES) 2010 emissions model with a 2010 mixed-light/heavy-duty fleet in Portland. In the present study, we estimate only CO_2, but other pollutants can be similarly modeled. For the base emissions rates we use $t(\lambda)$ as above (the BPR model) to relate λ to average speed – which is the input for the average-speed emissions model – with $t_o = 60\text{mph}$, $\lambda_c = 2{,}200$ vehicles per hour per lane (vphpl), $a = 0.15$ and $b = 7$.

We then apply a new emissions formulation which is similar to $t(\lambda)$, using four positive fitted parameters: $\alpha_0, \alpha_1, \alpha_2, n$, and nominal capacity λ_c:

$$\boldsymbol{e(\lambda) = \alpha_0 + \alpha_1\left(\lambda/\lambda_c\right) + \alpha_2\left(\lambda/\lambda_c\right)^n} \quad (2)$$

The fitted parameters are estimated by minimizing the square error of emissions rates with respect to base rates using λ as the independent variable, from 0 to 3,630 vehicles/hour/lane. This range of λ covers an average speed range from 10 to 60 mph. Fitting this curve, we find n to be about 10. This fitting gives us an R^2 of 0.996. Similar fitting is obtained for another emission model proposed by Barth and Boriboonsomsin (2008). The fitted parameters are shown in Table 1, and the fits are illustrated in Figure 1. The difference in magnitude of modeled emissions is to be expected, as the MOVES model includes heavy vehicles while the Barth model does not. Still, the $e(\lambda)$ formulation fits well for each modeled fleet.

Table 1. Fitted CO_2 Emissions Equation Parameters

Parameter	MOVES Estimate	Barth Estimate
$\boldsymbol{\alpha_0}$	0.4043	0.3253
$\boldsymbol{\alpha_1}$	0.02793	0.0000
$\boldsymbol{\alpha_2}$	0.003650	0.002641
$\boldsymbol{n}$	9.993	9.992

Assuming CO_2 emissions are directly proportional to fuel consumption, we can use the CO_2 emissions formulation to estimate both CO_2 emissions and fuel consumption. Using a fuel carbon intensity F of 10kgCO_2/gallon fuel (U.S. Environmental Protection Agency, 2009a), we have the fuel consumption $f(\lambda)$, in gallons/vehicle mile:

$$\boldsymbol{f(\lambda) = e(\lambda)/F = \left[\alpha_0 + \alpha_1 \left(\lambda/\lambda_c\right) + \alpha_2 \left(\lambda/\lambda_c\right)^n\right]/F} \quad (3)$$

Alternatively, fuel consumption could be modeled as a function of average travel speed and fit with a new set of parameters, as was done for emissions above.

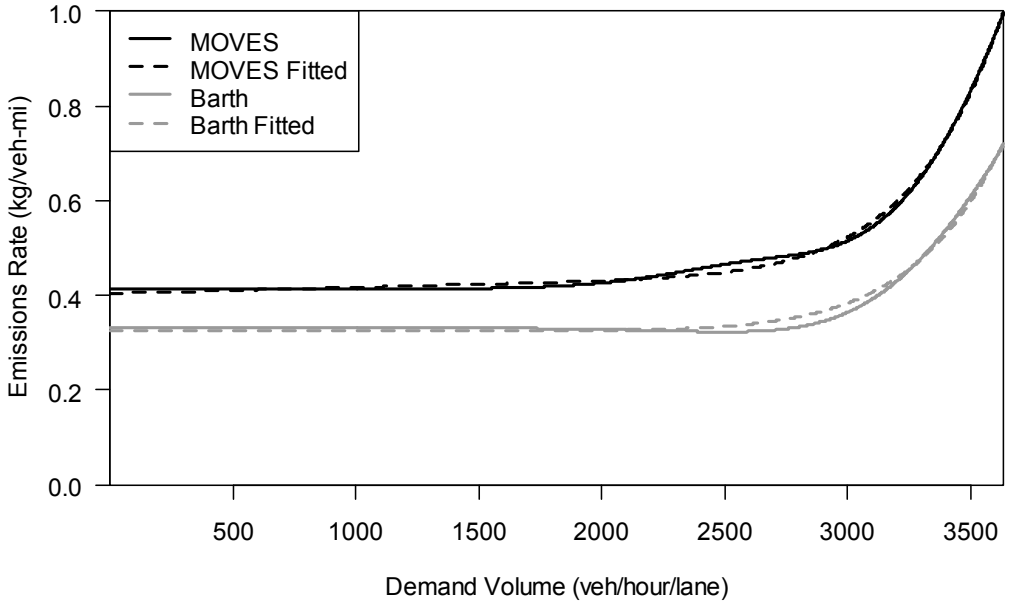

Figure 1. Emissions fit for MOVES (black) and Barth (grey) models

Total Costs and Benefits. Accounting for time, fuel and emissions costs, the total costs per unit of analysis time of flow rate λ are, in dollars/hour:

$$\boldsymbol{TC(\lambda) = c_t t(\lambda) l\lambda + c_f f(\lambda) l\lambda + c_e e(\lambda) l\lambda} \quad \textbf{(4)}$$

Introducing an inelastic demand function such that each trip on the segment has an associated benefit βl [dollars/vehicle] where $\beta > 0$ [dollars/vehicle mile], we can calculate the net social benefit per unit time of flow rate λ as:

$$\boldsymbol{NB(\lambda) = \beta l\lambda - c_t t(\lambda) l\lambda - c_f f(\lambda) l\lambda - c_e e(\lambda) l\lambda} \quad \textbf{(5)}$$

in dollars/hour. If we define a modified emissions cost coefficient $c_\varepsilon = c_e + c_f/F$, we can notate the net benefits simply as $NB(\lambda) = \beta l\lambda - c_t t(\lambda) l\lambda - c_\varepsilon e(\lambda) l\lambda$. The cost coefficient c_ε could also be further modified to take into consideration the cost of local pollutants (assuming their emissions are roughly proportional to CO_2 emissions).

2.2 STOCHASTIC FREEWAY CAPACITY

The previous analysis assumes the travel speed is a function of the volume of vehicles, but that traffic does not break down at any moment. Research has shown that after flow breakdown (a stochastic event), the traffic-flow characteristics are altered (Zhang and Levinson, 2004). Here we consider the case of a probabilistic breakdown in flow as traffic nears the roadway capacity.

Probability of Breakdown. We define $p(\lambda)$ as the traffic-flow breakdown, Bernoulli-probability function, where the mean of the probability of failure is a function of λ. From Brilon, Geistefeldt and Regler (2005), we can formulate the relationship as a Weibull-distributed cumulative distribution function:

$$\boldsymbol{p(\lambda) = 1 - e^{-\left(\frac{\lambda}{\varphi}\right)^{\omega}}} \quad \textbf{(6)}$$

where ω and φ are shape and scale parameters, respectively. They studied a three-lane German motorway and found $\omega \approx 13$ consistently, while φ ranged from about 1,650 to 2,200 vphpl for a one-hour, steady-flow interval. This agrees with recent research on flow breakdown on an urban freeway in Portland (Figliozzi and Saberi, 2011) – see Figure 2.

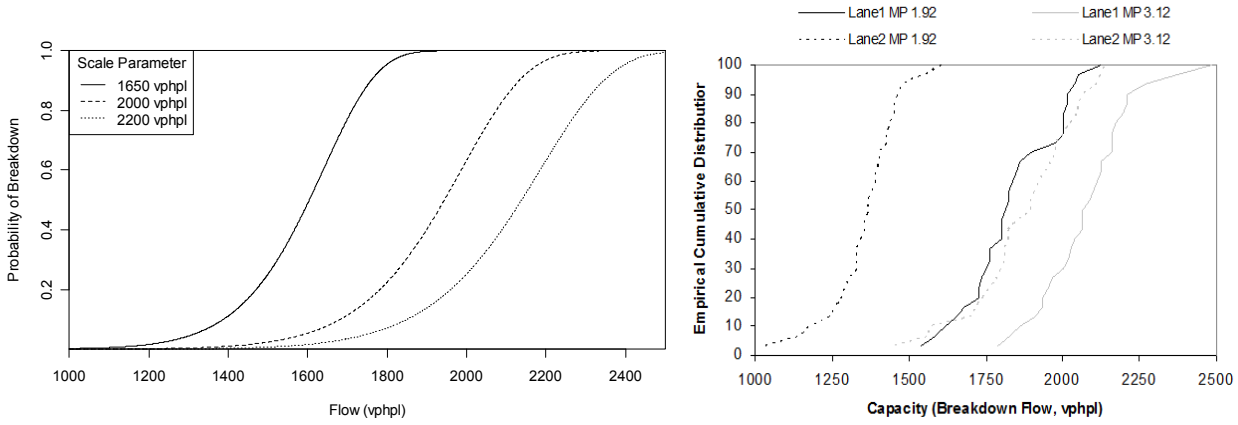

(a) (b)

Figure 2. Comparison of empirical breakdown probabilities from a) Brilon, et al. (2005) and b) Figliozzi and Saberi (2011)

Bottleneck Analysis. Assume that once flow breakdown occurs, a bottleneck is activated behind which a queue of slow-moving vehicles forms. This queue persists partly because of reduced throughput capacity after flow breakdown. If we assume a simple triangular shape on the space-time (*x*-*t*) plane for the extent of the bottleneck, we can estimate delay, fuel consumption and emissions after flow breakdown using some additional parameters. We define the following parameters, illustrated in Figure 3:

T: duration of time where a bottleneck (*bn*) is present, from $t = 0$

v_f: free-flow traffic speed outside the queue (equal to $v(\lambda)$ for $\lambda < \lambda_c$)

v_b: traffic speed in the queue, where $v_f > v_b$

v_w: speed of queue propagation (a *negative* number)

$v_{w'}$: speed of queue dissipation

l: length of the freeway section under study

The dashed lines in Figure 3 are idealized vehicle trajectories, representing average traffic speed as constant-speed vehicles.

Assume that a vehicle starts at the upstream end of the freeway section under consideration at a time τ with respect to the start of a bottleneck at the downstream end of the section, such that $0 \leq \tau + {}^{l}/_{v_f} \leq T$ in order to encounter the queue. The vehicle that reaches the queue at the initial activation of the bottleneck departs at time $\tau = -t_f$, where $t_f = {}^{l}/_{v_f}$. The vehicle that reaches the queue at the transition from formation to recovery wave of the bottleneck departs at time $\tau = t_r$, where $t_r = \frac{Tv_{w\prime}(v_w - v_f)}{v_f(v_w - v_{w\prime})} - \frac{l}{v_f}$. The last vehicle to encounter the bottleneck departs at time $\tau = t_e$, where $t_e = T - {}^{l}/_{v_f}$.

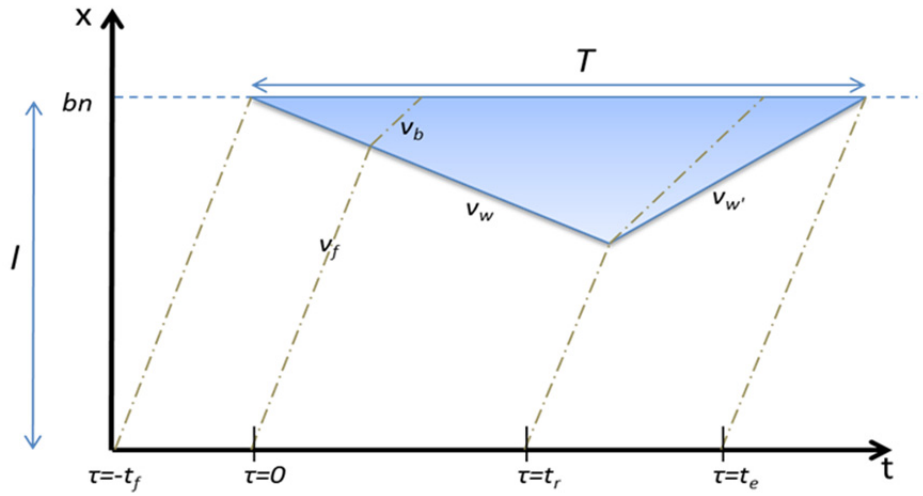

Figure 3. Illustrated breakdown flow parameters on the space-time plane

The travel time over the freeway segment for vehicles encountering the queue during formation (the propagation wave), where $-t_f \leq \tau \leq t_r$, is:

$$\boldsymbol{t_1 = \frac{l}{v_b} \cdot \frac{v_b - v_w}{v_f - v_w} + \tau \cdot \frac{v_w}{v_b} \cdot \frac{v_b - v_f}{v_f - v_w}} \quad \textbf{(7)}$$

and the travel time for vehicles encountering the queue during dissipation (the recovery wave), where $t_r \leq \tau \leq t_e$, is:

$$\boldsymbol{t_2 = \frac{l}{v_b} \cdot \frac{v_b - v_{w\prime}}{v_f - v_{w\prime}} + (T - \tau) \cdot \frac{v_{w\prime}}{v_b} \cdot \frac{v_f - v_b}{v_f - v_{w\prime}}}. \quad \textbf{(8)}$$

The travel time during the queue existence is then a piecewise linear function of the vehicle's departure time from the start of the section, with a maximum travel time for vehicles departing at t_r. These vehicles experience the maximum delay $D_{max} = l_{q\_max}\left(\frac{1}{v_b} - \frac{1}{v_f}\right)$, where max queue

length $l_{q\_max} = \frac{T v_w v_{w\prime}}{v_w - v_{w\prime}}$, and a travel time of $t_{max} = t_f + D_{max}$. The delay in the queue, averaged over time for vehicles encountering the queue, is $\overline{D} = {}^{D_{max}}/_{2}$.

Assume that if there is a bottleneck, the duration of the bottleneck $T = \delta\Delta$ where Δ is the time period of study with constant demand λ maintained, and $0 \leq \delta \leq 1$ is a coefficient that indicates the relative duration of the bottleneck in the period of study Δ. The average travel rate (time/distance) during Δ accounting for bottleneck delay is then:

$$\boldsymbol{t_b(\lambda) = t(\lambda) + \delta \frac{\overline{D}}{l} = \frac{\delta \cdot l_{q\_max}}{2 l v_b} + t(\lambda)\left(1 - \frac{\delta \cdot l_{q\_max}}{2l}\right)} \quad \textbf{(9)}$$

since $v_f = {}^{1}/_{t(\lambda)}$. Substituting for l_{q_max}, T, and $t(\lambda)$ we get:

$$\boldsymbol{t_b(\lambda) = t_o + \frac{\delta^2 \Delta v_w v_{w\prime}(1 - t_o v_b)}{2 l v_b (v_w - v_{w\prime})} + t_o a\left[1 - \frac{\delta^2 \Delta v_w v_{w\prime}}{2 l (v_w - v_{w\prime})}\right]\left({}^{\lambda}/_{\lambda_c}\right)^b} \quad \textbf{(10)}$$

which is a function of λ, with parameters $l, \delta, \Delta, v_w, v_{w\prime}, v_b, t_o, a, b,$ and λ_c and physical constraints $l_{q\_max} \leq l$ (the queue must be contained in the segment) and ${}^{1}/_{v_b} \geq t(\lambda)$ (the queue speed must be less than the un-queued speed). We can simplify the notation with a new dimensionless parameter:

$$\boldsymbol{\theta = \frac{\delta l_{q\_max}}{2l} = \frac{\delta^2 \Delta v_w v_{w\prime}}{2l(v_w - v_{w\prime})}} \quad \textbf{(11)}$$

which indicates the fractional effective bottleneck length in the context of the study period and road-segment length. Using θ:

$$\boldsymbol{t_b(\lambda) = \frac{\theta}{v_b} + (1 - \theta) \cdot t(\lambda)} \quad \textbf{(12)}$$

and the average travel rate if flow breakdown occurs is a function of λ with parameters $\theta, v_b, t_o, a, b,$ and λ_c.

Using (1) and (2), the average emissions rates e_q (per vehicle, per mile) for vehicles inside a queue with average speed v_b can be estimated as:

$$\boldsymbol{e_q = e\left(\lambda_c \left(\frac{1 - v_b t_o}{v_b t_o a}\right)^{1/b}\right) = \alpha_0 + \alpha_1 \left(\frac{1 - v_b t_o}{v_b t_o a}\right)^{1/b} + \alpha_2 \left(\frac{1 - v_b t_o}{v_b t_o a}\right)^{n/b}} \quad \textbf{(13)}$$

with parameters $a, b, t_o, \alpha_0, \alpha_1, \alpha_2,$ and n. The emissions for vehicles outside the queue is the same as $e(\lambda)$. Neglecting the transitions in/out of the queue, by a parallel process as the development of (12) we can estimate the emissions when a bottleneck occurs as:

$$\boldsymbol{e_b(\lambda) = \theta \cdot e_q + (1 - \theta) \cdot e(\lambda)} \quad \textbf{(14)}$$

If we estimate the excess queue-transition emissions for a vehicle entering and exiting the queue as $\boldsymbol{e_t}$ in mass per vehicle encountering the queue, then the average emissions rate after breakdown (per vehicle, per mile) becomes:

$$\boldsymbol{e_b(\lambda) = \theta \cdot e_q + (1 - \theta) \cdot e(\lambda) + \frac{\delta}{l} \cdot e_t} \quad \textbf{(15)}$$

The equations for $e_b(\lambda)$ and $t_b(\lambda)$ are linear functions of $e(\lambda)$ and $\mathrm{t}(\lambda)$. We can estimate the size of e_t using an assumption of constant deceleration/acceleration for vehicles encountering the queue. Let the emissions rates (per vehicle mile) with constant acceleration a and constant deceleration d be e_a and e_d, respectively, and free-flow emissions be e_f. Then the *excess* emissions in mass per vehicle during the transitions are:

$$\boldsymbol{e_t = \frac{v_b^2 - v_f^2}{2d}\left(e_d - e_f\right) + \frac{v_f^2 - v_b^2}{2a}\left(e_a - e_f\right).} \quad \textbf{(16)}$$

Long (2000) discusses various acceleration characteristics of vehicles, and cites NCHRP (National Cooperative Highway Research Program) Report 270 for average accelerations around 2 mph/second in the 30-60 mph speed range (Olson et al., 1984). Assuming this value for both transition accelerations and decelerations, we modeled constant accelerations and decelerations in the 30-60 mph speed range using the project-level methodology of the MOVES 2010 emissions model (U.S. Environmental Protection Agency, 2009b), with the same fleet and other characteristics as above from Bigazzi and Figliozzi (2011). MOVES outputs for CO_2 generated, on average, $e_a = 0.957$ kg/vehicle mile and $e_d = 0.156$ kg/vehicle mile. Using $e_f = 0.404$ kg/vehicle mile at 60 mph free-flow speed (see Table 1), these lead to:

$$\boldsymbol{e_t = 2.12 \times 10^{-5}\left(v_f^2 - v_b^2\right)} \quad \textbf{(17)}$$

with speeds in mph and e_t in kg/vehicle. For free-flow speed of 60 mph and queued speeds in the 10-40 mph range, this results in an equivalent emissions-distance penalty of $d_e = \frac{e_t}{e_f} = 0.10$ to 0.18 miles (the distance at free-flow speed that produces the same amount of excess emissions as those produced by the queue transition).

Modified Cost Functions. Utilizing the probabilistic function $p(\lambda)$ we generate the revised travel rate function:

$$\begin{aligned} \boldsymbol{t'(\lambda)} &= \boldsymbol{p(\lambda) \cdot t_b(\lambda) + \left(1 - p(\lambda)\right) \cdot t(\lambda)} \\ &= \boldsymbol{t(\lambda) + p(\lambda)\theta\left[\frac{1}{v_b} - t(\lambda)\right]} \end{aligned} \quad \textbf{(18)}$$

Similarly, the revised average emissions rate function is:

$$\begin{aligned} \boldsymbol{e'(\lambda)} &= \boldsymbol{p(\lambda) \cdot e_b(\lambda) + \left(1 - p(\lambda)\right) \cdot e(\lambda)} \\ &= \boldsymbol{e(\lambda) + p(\lambda)\left[\theta\left(e_q - e(\lambda)\right) + \frac{\delta}{l} e_t\right]} \end{aligned} \quad \textbf{(19)}$$

The fuel-consumption estimate can also be revised as per (3) using $e'(\lambda)$ for $e(\lambda)$. For net social benefits considering probabilistic flow breakdown, we then have:

$$\boldsymbol{NB'(\lambda) = \beta l\lambda - c_t t'(\lambda) l\lambda - c_\varepsilon e'(\lambda) l\lambda} \quad \textbf{(20)}$$

where $c_\varepsilon = c_e + c_f/F$.

The *value of reliability* (or cost of unreliability) with respect to traffic-flow instability is defined as the decrease in social benefit due to stochastic freeway capacity. In units of dollars/hour of analysis:

$$\begin{aligned} \boldsymbol{VR(\lambda)} &= \boldsymbol{c_t l\lambda[t'(\lambda) - t(\lambda)] + c_\varepsilon l\lambda[e'(\lambda) - e(\lambda)]} \\ &= \boldsymbol{\lambda l\theta p(\lambda)\left[c_t\left[\frac{1}{v_b} - t(\lambda)\right] + c_\varepsilon\left[e_q - e(\lambda) + \frac{\delta}{\theta l} e_t\right]\right]} \end{aligned} \quad \textbf{(21)}$$

This can be put into units of dollars/vehicle mile by dividing by l and λ. So the value of reliability (related to stochastic capcity) can be estimated as a function of λ with parameters of section length, the cost coefficients (except β), the breakdown-probability function, the bottleneck parameters, the BPR parameters, the emissions-formulation parameters, and the queue-transition emissions.

3.0 CASE STUDY

We now present a case-study application using archived loop-detector data from OR 217, a congested freeway corridor in the Portland metro region. The parameter values for use in the above equations and their sources are shown in Table 2. Much of the data come from PORTAL, a transportation data archive at Portland State University: http://portal.its.pdx.edu. The freeway stochastic-capacity data come from Figliozzi and Saberi (2011), who recently analyzed traffic characteristics on this corridor utilizing PORTAL data.

From (6), we can estimate φ to make the likelihood of breakdown at nominal capacity a certain value p_c, $p(\lambda_c) = p_c$ using $\varphi = \lambda_c \left[ln\left({}^{1}/_{1-p_c}\right)\right]^{-{}^{1}/_{\omega}}$. For a median value of $p_c = 0.5$, $\varphi_{0.5} = 1.0286\lambda_c$, for $p_c = 0.90$, $\varphi_{0.9} = 0.9379\lambda_c$. Here we assume the nominal capacity (used in the BPR equation) equates to a 90% likelihood of flow breakdown, $p_c = 0.90$. We initially assume travel benefits $\beta = \$0.50$ per vehicle mile. Theta, a function of the breakdown flow parameters (Δ, δ, v_w, and $v_{w'}$) and segment length l – see (11), is calculated from the parameters in Table 2 as 0.27; the corresponding maximum queue length is 4.8 miles.

Table 2. Parameters Used in the Case Study

Parameter	Value	Units	Source
l	7	mi	Roadway
Δ	1	hours	approximated from PORTAL data
δ	0.8	-	approximated from PORTAL data
FFS	60	mph	approximated from PORTAL data
a	0.15	-	(Figliozzi and Saberi, 2011)
b	7	-	(Figliozzi and Saberi, 2011)
λ_c	2200	vphpl	(Figliozzi and Saberi, 2011)
v_b	26	mph	(Figliozzi and Saberi, 2011)
v_w	-12	mph	(Lu and Skabardonis 2007; Castillo and Benítez 1995)
$v_{w'}$	12	mph	assumed to be the same as v_w
ω	13	-	(Brilon, Geistefeldt, and Regler 2005)
φ	2063	vphpl	Makes λ_c the 90th percentile from (6), see above
e_t	Eq'n (**17**)	kg/veh	MOVES2010 modeling (see above)
c_t	15	$/veh-hr	assumed from (Schrank and Lomax 2009)
c_e	0.02	$/kg CO_2	assuming US$20/tonne CO_2, from EU ETC
c_f	3	$/gal	assumed from (Schrank and Lomax 2009)
F	10	kgCO_2/gal	(U.S. Environmental Protection Agency 2009a)

$\boldsymbol{\beta}$	0.50	\$/veh-mi	Assumed

3.1 NET BENEFITS, OPTIMAL FLOW, AND THE VALUE OF RELIABILITY

The results of applying the parameters in Table 2 to calculate net benefits as embodied in (**20**) are shown below. The cost components, total costs, benefits, and net benefits are illustrated in Figure 4. The total costs are dominated by travel-time costs, and emissions costs are negligible. All cost components increase more rapidly as the flow approaches capacity and the likelihood of flow breakdown increases. The optimal flow here to maximize net benefits is 1,658vphpl (75% of λ_c).

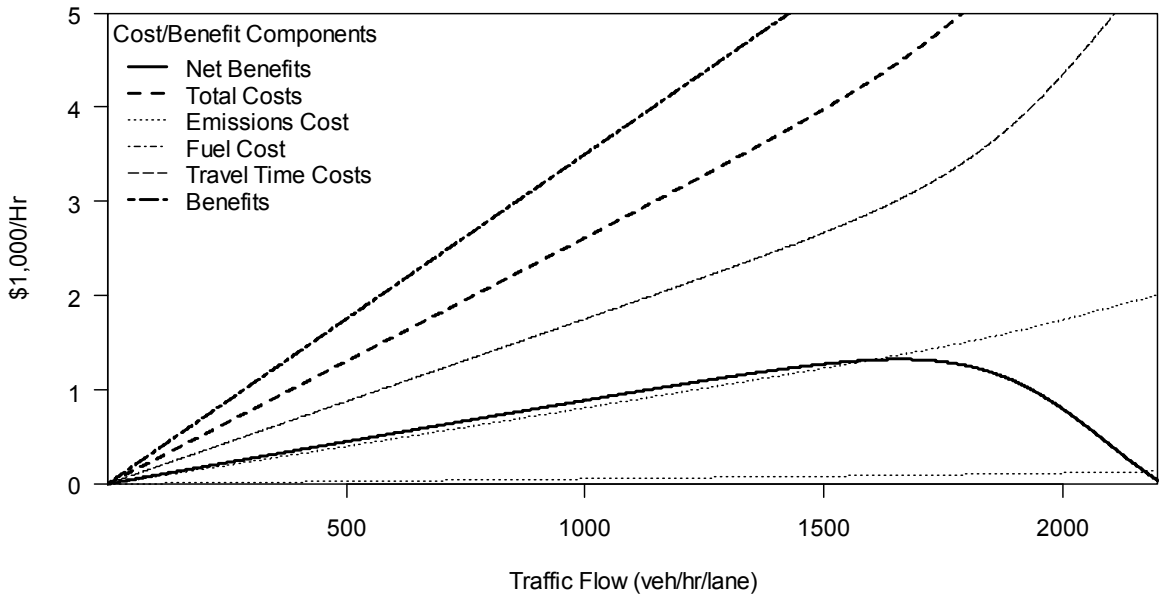

Figure 4. Case-study cost and benefit curves

The parameter with the highest uncertainty is β, which would require some knowledge of the trips and travelers to estimate accurately. This parameter impacts both net benefits and the optimal flow rate. Given this uncertainty, it is interesting (and perhaps most useful) to look at how optimal flows vary with β. To this end, Figure 5 illustrates the impacts of varying β on optimal flow. Figure 5 also shows the impacts of the probabilistic breakdown formulation with two different optimal-flow curves – with and without considering $p(\lambda)$.

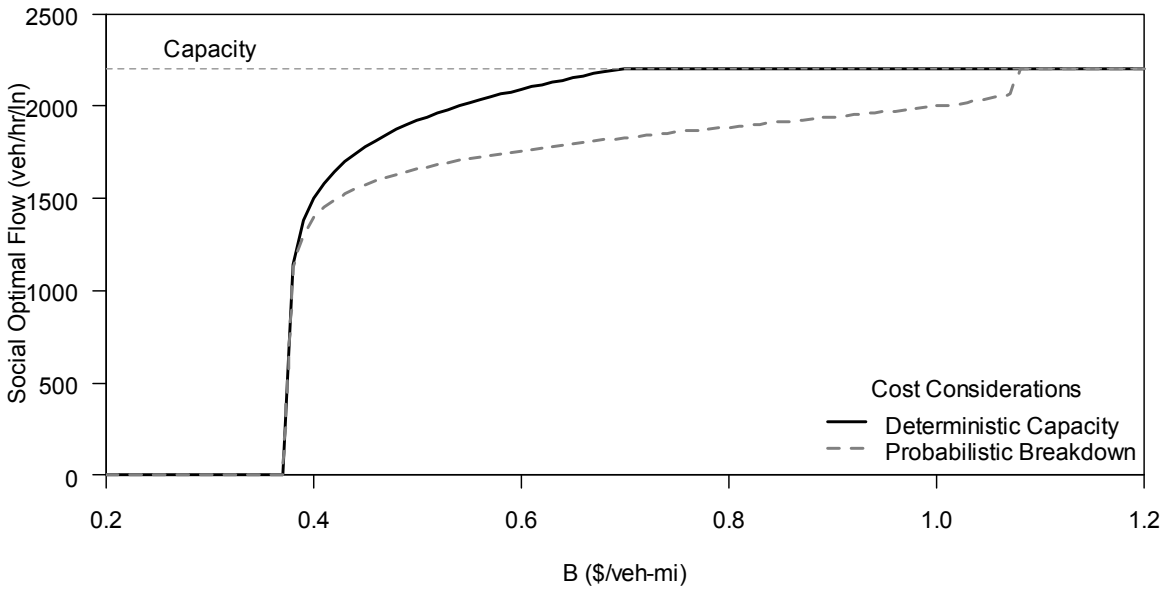

Figure 5. Impact of considering probabilistic breakdown on optimal flows

Here we see that there is an initial per-mile benefit threshold, below which auto travel is not worthwhile. For β just above this threshold, optimal flows quickly rise to the lower probabilities of breakdown flow, around 1,400 vphpl (which equates to $p(1400) = 0.01$). As β increases, higher flows are optimal because the value of additional trips outweighs the increased marginal costs for all vehicles. Optimal flows increase more slowly with β when using the probabilistic formulation, which considers the possibility of flow breakdown below capacity. Using stochastic costs, a doubling of the benefits of travel from \$0.40 to \$0.80/vehicle mile results in an optimal flow increase of only about 30%, while the deterministic curve increases to capacity (more than 45%). Lower optimal flows reduce the likelihood of flow breakdown at the sacrifice of additional throughput; up to $\beta = \$0.80$/vehicle mile the optimal flow is still below $p(\lambda) = 0.27$. The optimal flow difference between the curves in Figure 5 shows that reducing $p(\lambda)$ is a key factor to increasing optimal traffic-flow volumes.

As the optimal flow rates approach the roadway capacity where breakdown is nearly certain, there is a "Capacity Point" for β at which, despite the increased costs of queued conditions, the value of travel supersedes flow restrictions. This occurs at around \$0.70/vehicle mile considering deterministic costs and \$1.06/vehicle mile considering stochastic costs. The "Capacity Point" considering probabilistic breakdown is 50% greater than for deterministic conditions – indicating that trip values must be much higher in order to warrant high volumes if we consider traffic instability below the capacity threshold. For probabilistic breakdown, there is a sudden change in the optimal flow curve as traffic flows near capacity that reflects the flattening of the Weibull distribution near capacity flows (see Figure 2).

The value of reliability (or cost of unreliability), here computed by (**21**), increases with $p(\lambda)$ as we approach the roadway capacity. The marginal social value of reliability increases from

essentially zero at flows below 1,500 vphpl to about \$0.08/vehicle mile at flows just below capacity. This value of reliability is about 16% of total estimated stochastic costs (per vehicle mile) near capacity for the study corridor. The value of reliability is alternatively expressed as \$0.56 per vehicle throughput on the segment, since it is negligibly sensitive to segment length. As a reminder, this is only the unreliability due to stochastic capacity, not due to crashes or other incidents.

Finally, Figure 6 presents optimal flows versus β when considering different combinations of cost components. While emissions costs are negligible (at present valuations), the impacts of considering fuel costs are substantial. For example, the "Capacity Point" for total costs is about 20% higher than when neglecting fuel costs. In the other dimension, at $\beta = \$0.80$/vehicle mile the optimal flow is about 5% lower when considering fuel costs as compared to neglecting them.

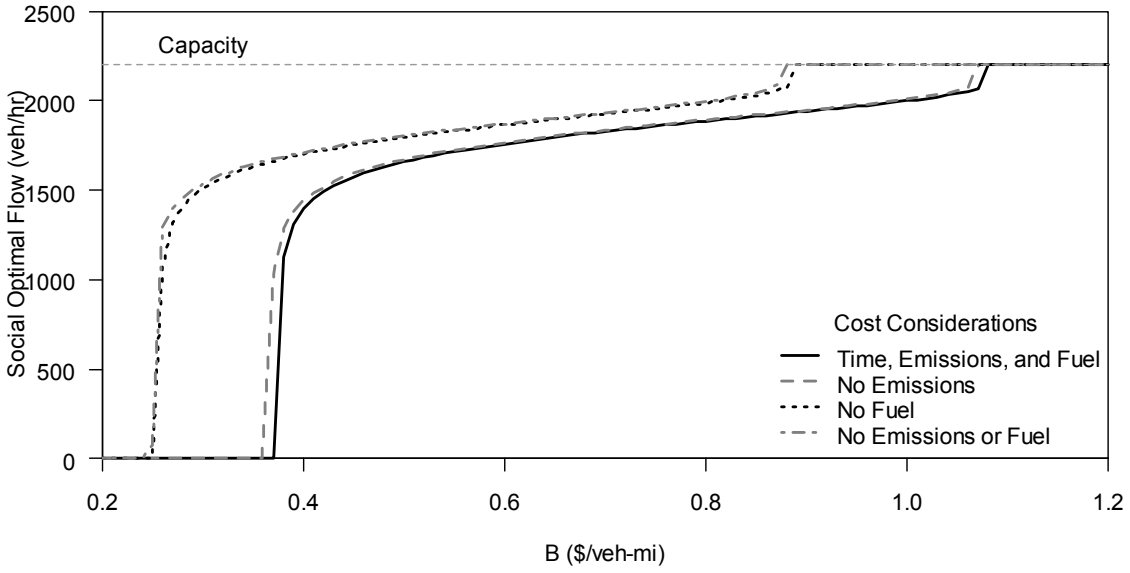

Figure 6. Optimal flow versus β, with different cost components

3.2 CASE-STUDY SENSITIVITY

Elasticities of net benefits, optimal flows, and the value of reliability to changes in various parameters were calculated, as presented in Table 3. The elasticity is the percent change in the dependent variable (benefit/flow/reliability) with each percent change in the parameter value, with respect to initial parameter values from Table 2. The initial optimal flow is 1,658 vphpl with the initial net benefit of \$1,323/hour estimated at this optimal flow. The initial value of reliability is estimated at capacity flow (2,200 vphpl) as \$1,273/hour.

The cost coefficient for time and the benefits per mile (c_t and β) are important factors for net benefits. The free-flow speed is also important for net benefits as it greatly impacts the travel time on the segment. Optimal flow is generally much less sensitive to parameters than net benefits are, though c_t and β are still among the more important factors. The scale parameter of the breakdown probability function φ is the most important factor for optimal flow, which is to

be expected from the importance of flow-breakdown likelihood illustrated in Figure 5. The value of reliability is most impacted by bottleneck characteristics such as δ and v_b, as well as the breakdown-probability scale parameter φ.

Table 3. Elasticities of Net Benefits, Optimal Flow, and the Value of Reliability to Parameters

Parameter	Net Benefit Elasticity	Optimal Flow Elasticity	Value of Reliability Elasticity
L	1.00	0.06	0.00
Δ	-0.05	-0.07	0.90
δ	-0.09	-0.13	**1.66**
FFS	**2.00**	0.17	0.83
a	-0.04	-0.03	-0.11
b	0.08	0.03	0.00
λ_c	0.32	0.20	0.76
v_b	0.08	0.11	**-1.67**
v_w	-0.03	-0.04	0.47
v_w,	-0.03	-0.04	0.47
ω	0.12	0.10	0.00
φ	0.55	0.71	**-2.50**
e_t	0.00	0.00	-0.02
θ	-0.05	-0.07	0.90
c_t	**-2.00**	-0.28	0.83
c_e	-0.07	0.00	0.01
c_f	-1.00	-0.10	0.13
β	**3.33**	0.38	0.00

3.3 AGGREGATE ANALYSIS ACROSS URBAN AREAS

Our final analysis applies the previous concepts to urban areas. This aggregate or macro analysis attempts to find a relationship between urban congestion characteristics, size, density and traffic flows. To do this, we gather macroscopic characteristics of peak-period freeway volumes in different cities from the data tables of the Texas Transportation Institute's 2009 Urban Mobility Report (UMR) (Schrank and Lomax, 2009). The urban areas selected are the most and least "traveler-dense" urban areas in the three top size categories: "Medium" (0.5-1 million people), "Large" (1-3 million), and "Very Large" (>3 million). Traveler density is assessed as the number of peak-period travelers per square mile, easily extractable from the UMR data tables.

From the UMR data tables we can estimate average peak-period trip distance on major facilities by dividing total peak-period freeway and arterial vehicle miles traveled (VMT) by the number of peak-period travelers. Since the number of travelers will exceed the number of vehicles, this is a low-end approach to estimating miles per person, per day. We also use the UMR data to calculate average congested, peak-period freeway volumes, in vehicles per hour per lane (vphpl), by assuming the portion congested (in VMT and lane miles) is equivalent on freeways and arterials, and an even directional split. For each urban area, the UMR provides estimates of freeway and arterial VMT and lane miles, fractions of VMT and lane miles congested, and number of "rush hours" - assumed to be congested. By assuming even distributions, this is a conservative approach to volume estimates. These assumptions provide an admittedly rough approximation, but one which can be used to illustrate the differences among urban areas. Table 4 shows the six urban areas analyzed along with their population, peak-period traveler density, percent of lane miles congested, average peak-period trip distance, and average congested peak-period freeway volume – all extracted or calculated from the UMR data tables for 2007.

Table 4. Urban Areas' Average Characteristics

Urban Area	Population	Peak Traveler Density	Lane-mi Congested	Peak Trip Distance	Peak Freeway Volume
	(1,000's)	(per mi^2)	(%)	(mi)	(vphpl)
Atlanta	4,440	771	58	19.5	1,570
Los Angeles	12,800	3,087	61	19.2	2,098
Raleigh-Durham	1,025	671	53	20.6	1,089
Las Vegas	1,405	2,539	53	16.4	1,700
Nashville	995	725	43	23.8	1,061
Honolulu	705	2,771	51	12.2	1,174

We use the urban area and congestion data to calculate the per-traveler dollar values per mile (β) that would justify capacity flows under deterministic and stochastic conditions. In addition, we calculate the per-traveler dollar values per mile (β) that would justify an optimal flow under deterministic and stochastic conditions. For θ in each urban area (the effective fraction of roadway in queued conditions after flow breakdown), we assume a value equal to the percent of lane miles congested during the peak period (Table 4), and for v_b we assume a value of 35 mph

(from the UMR methodology – see Appendix A of the UMR (Schrank and Lomax, 2009)). The other parameters for cost coefficients, $t(\lambda)$, $e(\lambda)$, and $p(\lambda)$ are assumed to be the same as above for the case study (bottleneck parameters do not apply since we are using θ).

Per-traveler dollar values per mile (β) that would justify capacity and optimal flows under deterministic and stochastic conditions are shown in Table 5. The per-traveler dollar values that justify capacity flows under deterministic conditions are the same across urban areas. However, if the costs associated to stochastic capacity are taken into account, the per-traveler dollar values increase with the urban area size and density. Percentagewise, the increase between deterministic and stochastic conditions ranges from 28-38%. To optimize existing flows, the per-traveler dollar values also increase with urban size and density. However, the increase associated with stochastic capacity is significant in the very large, high-density urban area. The increase between deterministic and stochastic conditions ranges from 0-46%. Hence, to optimally control traffic flows, it is especially important to consider stochastic capacity in large urban areas with high traffic density.

Table 5. Comparison of Per-Traveler Dollar Values Per Mile (β) Across Urban Areas

Urban Area	Urban Area Size	Traveler Density	β to justify capacity flow			β to optimize existing avg. peak-period freeway flows		
			Det.	**Sto.**	**% Change**	**Det.**	**Sto.**	**% Change**
Atlanta	Very Large	Low	$0.70	$1.10	36.4%	$0.41	$0.46	10.9%
Los Angeles		High	$0.70	$1.13	38.1%	$0.60	$1.12	46.4%
Raleigh-Durham	Large	Low	$0.70	$1.06	34.0%	$0.38	$0.38	0.0%
Las Vegas		High	$0.70	$1.06	34.0%	$0.43	$0.54	20.4%
Nashville	Mid Size	Low	$0.70	$0.98	28.6%	$0.38	$0.38	0.0%
Honolulu		High	$0.70	$1.04	32.7%	$0.38	$0.38	0.0%

Per-traveler dollar values (βl) of daily peak-period trips that would justify capacity and optimal flows under deterministic and stochastic conditions are shown in Table 6. Less-dense urban areas require higher trip values to warrant capacity flow since the trip lengths tend to be longer (which lowers value per mile). Conversely, for a given peak-period trip value, denser areas will have higher optimal flow rates because the β value is larger. This is particularly true for mid-sized urban areas, since the larger the population the less of a difference in trip distance is

observed for areas with different traveler densities. Though the changes in trip value that justify capacity flows are somewhat similar across urban areas, the change in trip value that justifies optimal flows is considerably larger in very large areas with high density.

Table 6. Comparison of Per-Traveler Trip Dollar Values (βl) Across Urban Areas

Urban Area	Urban Area Size	Traveler Density	βl to justify capacity flow			βl to optimize existing avg. peak-period freeway flows		
			Det.	**Sto.**	**$ Change**	**Det.**	**Sto.**	**$ Change**
Atlanta	Very Large	Low	$13.68	$21.49	$7.81	$8.01	$8.99	$0.98
Los Angeles		High	$13.43	$21.68	$8.25	$11.51	$21.49	$9.98
Raleigh-Durham	Large	Low	$14.44	$21.87	$7.43	$7.84	$7.84	$0.00
Las Vegas		High	$11.46	$17.35	$5.89	$7.04	$8.84	$1.80
Nashville	Mid Size	Low	$16.67	$23.33	$6.66	$9.05	$9.05	$0.00
Honolulu		High	$8.52	$12.66	$4.14	$4.62	$4.62	$0.00

These trip values can be interpreted as the "break-even" trip values, above which increasing freeway flows are still warranted, but below which the observed flows are inefficiently high. Again, the impact of stochastic capacity is significant in larger urban areas with higher traffic density. Finally, urban areas with low peak volumes (below 1,200 vphpl) have no observable difference between probabilistic and deterministic conditions, while those very near capacity (e.g., Los Angeles) are greatly affected by the uncertainty of breakdown conditions. The high likelihood of traffic-flow breakdown combined with long trip lengths makes the break-even trip value for existing conditions in Los Angeles double that of any other urban area when considering stochastic capacity.

As stated above, these comparisons by urban area are based on a set of some aggregate characteristics of the urban areas and peak-period travel. To see the sensitivity of these results, we varied these assumptions and the key parameters, as indicated by Table 3. Using the Portland case-study values for θ and v_b (both of which are lower) has no large impact on the results. Decreasing θ reduces stochastic costs at capacity and for high-volume areas, but decreasing v_b has the opposite (and, here, offsetting) effect. This suggests that these results are *intuitive* and *consistent* with varying thresholds of congestion.

Increasing the roadway capacity (or scale parameter of the probability of breakdown function) reduces the stochastic costs for high-volume areas since they are less exposed to congestion or flow breakdown. On the other hand, assuming less-homogenous flow distribution increases the

costs for higher-volume urban areas. Varying other parameters such as free-flow speed and cost coefficients has little to no effect on the comparison among urban areas. The ratio of stochastic to deterministic costs for each urban area similarly increases with parameters that increase congestion penalties. For observed volumes the stochastic/deterministic cost ratio ranges from 1.0 for low-volume areas to 1.9 for Los Angeles. This ratio tends to increase with higher volumes (which themselves increase with traveler density). Given the uncertainty in parameter estimation, the above results comparing urban areas are presented as conservative estimates, with the caveat that they are highly sensitive to assumptions about θ, v_b, and the directional split. The estimates are conservative in that they will tend to underestimate trip distances, peak volumes, and stochastic costs, as explained above. While the absolute cost estimates are highly sensitive to the assumptions, the same general trends in the results hold (though possibly magnified) for varying parameter values.

3.4 DISCUSSION

In the first section of this report, we model the costs and benefits of freeway traffic flows as a function of travel-time reliability (i.e., stochastic capacity). We apply this model to: (a) a congested freeway corridor in Portland using real-world archived traffic data and (b) six distinct urban areas across the U.S.

The freeway case-study results show that unreliability decreases optimal traffic-flow volume – and increases travel value that is required to justify flow at capacity. Travel time is the dominant cost, followed by fuel costs; emissions costs are negligibly small at present valuations. The value of reliability is most sensitive to the breakdown-flow characteristics, such as bottleneck travel speed, bottleneck duration, and the probability of traffic breakdown. A sensitivity analysis indicates that net social benefits and optimal flow are most sensitive to the travel-time cost coefficient, the travel benefit coefficient, and the free-flow speed.

Comparing macroscopic peak-period traffic characteristics among urban areas of varying size and density, results are intuitive and consistently indicate that the impacts of stochastic capacity are more significant in larger and denser urban areas. The large and dense urban areas have markedly higher flows, which increase the marginal costs of travel and can offset shorter trip lengths when estimating net benefits. These results indicate that there is a tradeoff between trip length and traffic intensity in urban areas with different density.

4.0 STRATEGIES TO MITIGATE CONGESTION AND EMISSIONS

Policymakers, researchers and activists often assume that congestion reductions inevitably lead to reduced vehicle emissions. In many cases, emissions reductions are cited as an implicit benefit of congestion mitigation without proper justification or quantification of the benefits. For example, the U.S. Federal Highway Administration's Congestion Mitigation and Air Quality (CMAQ) Improvement Program suggests a clear co-beneficial relationship between the two. The CMAQ program has provided over $14 billion in funding since 1991 for transportation projects to improve air quality and reduce congestion (Federal Highway Administration, 2010) – one third of it for traffic-flow improvement projects (Transportation Research Board, 2002; Grant et al., 2008). If congestion mitigation is to be tied to air-quality goals, we need a better understanding of total congestion impacts on motor-vehicle emissions.

Vehicle emissions have an established role in decreasing urban air quality and increasing atmospheric greenhouse gases. Concurrently, roadway congestion impacts urban areas throughout the world with varying economic, social and environmental costs. But the full effects of traffic congestion on motor-vehicle emissions are still not well quantified due to the existence of feedback effects and complex interactions. Potential changes in travel behavior or vehicle technology are two factors that complicate the evaluation of congestion-mitigation effects on future emissions.

An important consideration to evaluate the impact of congestion-mitigation measures on emissions is the effect of induced travel-demand volume resulting from travel-time savings. A report by Dowling (2005) used travel-demand modeling to estimate the air-quality effects of traffic-flow improvements. The conclusion of the report states that more research is needed "to better understand the conditions under which traffic-flow improvements contribute to an overall net increase or decrease in vehicle emissions." Other, more focused research on a limited spatial scale has shown that induced demand from individual traffic-flow improvements can entirely offset emissions-rate reductions (Stathopoulos and Noland, 2003; Noland and Quddus, 2006).

Capacity-based strategies (CBS) for reducing emissions ease congestion by increasing a roadway's vehicle throughput capacity and increasing vehicle operating efficiency. CBS can increase capacity by increasing lane miles or by increasing existing roadway utilization through traffic-flow improvements. The desired emissions benefit of congestion mitigation through CBS is reduced marginal emissions rates at higher average traffic speeds. However, CBS have the potential to generate induced vehicle-travel demand.

Alternative strategies for reducing emissions can be based on more efficient vehicles – efficiency-based strategies (EBS) – or on reduced vehicle travel demand – demand-based strategies (DBS). EBS directly target emissions through cleaner vehicles and fuels or more efficient driving. DBS, such as road pricing, reduce emissions by reducing vehicle-travel volume and can reduce congestion simultaneously.

In this paper we investigate the broad conditions in which emissions co-benefits can be expected from congestion mitigation and compare capacity-, efficiency-, and demand-based emissions reduction strategies. In particular, the paper studies the effects of travel-demand elasticity, the consequences of more efficient vehicles in the fleet, and the role of light-duty and heavy-duty vehicles across different types of pollutants. The methodological framework used in this paper allows for a parsimonious estimation of net emissions effects at the aggregated level. This framework is presented in the next section.

5.0 METHODOLOGICAL FRAMEWORK TO COMPARE STRATEGIES

This section describes the notation and equations used in this paper to investigate tradeoffs among travel speed, travel volume and total emissions. The concept of elasticity is employed to set up the conditions that lead to positive or negative net emissions changes. The elasticity, $\varepsilon_{\bar{e}}^{\bar{v}}$, of average emissions rate, $\bar{e}$, to average travel speed, $\bar{v}$, is expressed:

$$\boldsymbol{\varepsilon_{\bar{e}}^{\bar{v}} = \frac{\bar{v}}{\bar{e}} \cdot \frac{\partial \bar{e}}{\partial \bar{v}}.} \qquad \textbf{(22)}$$

The average vehicle-emissions rate in mass per unit distance of travel is denoted as $\bar{e}$, and total emissions from all on-road vehicles in mass per unit length of road, per unit of time is denoted as E. If the total travel-demand volume on a roadway is q (in vehicle throughput per unit time), then $E = q \cdot \bar{e}$. The average travel speed on the roadway is denoted as $\bar{v}$, in distance traveled per unit time.

The *long-term* elasticity of travel-demand volume q to average speed $\bar{v}$ is expressed:

$$\boldsymbol{\eta_q^{\bar{v}} = \frac{\bar{v}}{q} \cdot \frac{\partial q}{\partial \bar{v}}.} \qquad \textbf{(23)}$$

The value of $\eta_q^{\bar{v}}$ represents the percentage change in vehicle miles traveled (VMT) with a 1% $\bar{v}$ change on a roadway of arbitrary length. The elasticity of E to $\bar{v}$ is then:

$$\boldsymbol{\varepsilon_E^{\bar{v}} = \frac{\bar{v}}{E} \cdot \frac{\partial E}{\partial \bar{v}} = \frac{\bar{v}}{q \cdot \bar{e}} \left(\frac{\partial q}{\partial \bar{v}} \cdot \bar{e} + q \cdot \frac{\partial \bar{e}}{\partial \bar{v}} \right) = \eta_q^{\bar{v}} + \varepsilon_{\bar{e}}^{\bar{v}}.} \qquad \textbf{(24)}$$

This relationship, $\varepsilon_E^{\bar{v}} = \eta_q^{\bar{v}} + \varepsilon_{\bar{e}}^{\bar{v}}$, is the central equation of the methodological framework; it expresses the elasticity of total emissions to average travel speed as the combined effects of changes in travel-demand volumes and emission rates. The break-even demand elasticity to speed, denoted $\gamma_q^{\bar{v}}$, that produces the condition $\varepsilon_E^{\bar{v}} = 0$ is $\gamma_q^{\bar{v}} = -\varepsilon_{\bar{e}}^{\bar{v}}$. It follows that:

$$\varepsilon_E^{\bar{v}} = \eta_q^{\bar{v}} - \gamma_q^{\bar{v}}, \qquad (25)$$

the difference between true demand elasticity and break-even demand elasticity is the total emissions elasticity to speed.

The preceding equations are for an aggregate vehicle fleet; to understand the impacts of different vehicle classes, additional notation and formulae are needed. For vehicles of class j (in the mutually exclusive and exhaustive set of vehicle classes J), the average emissions rate is e_j and travel-demand volume is q_j. The fraction of on-road vehicles that are of class j (by distance

traveled) is f_j, so that $f_j = \frac{q_j}{q}$. Class-total emissions are $E_j = q_j \cdot e_j = q \cdot f_j \cdot e_j$, and the elasticities $\varepsilon_{E_j}^{v_j}$, $\eta_{q_j}^{v_j}$, and $\varepsilon_{e_j}^{v_j}$ are similar to the ones defined previously, but only for vehicles of class j. Total emissions, E, from on-road vehicles of all classes in J, per unit length of road per unit time, are the sum of each class's total emissions $E = \sum_{\mathrm{j}\in\mathrm{J}} E_j = \sum_{\mathrm{j}\in\mathrm{J}}(q_j \cdot e_j)$. From this:

$$\boldsymbol{E = q \cdot \sum_{\mathrm{j}\in\mathrm{J}}(f_j \cdot e_j) = q \cdot \bar{e}\ .} \tag{26}$$

Employing $\varepsilon_{E_j}^{v_j} = \frac{v_j}{E_j} \cdot \frac{\partial E_j}{\partial v_j}$, the elasticity of E to $\bar{v}$ considering distinct vehicle classes is:

$$\varepsilon_E^{\bar{v}} = \frac{\bar{v}}{E} \cdot \frac{\partial \sum_{\mathrm{j}\in\mathrm{J}} E_j}{\partial \bar{v}} = \frac{\bar{v}}{E} \cdot \sum_{\mathrm{j}\in\mathrm{J}} \left[\frac{\partial E_j}{\partial v_j} \cdot \frac{\partial v_j}{\partial \bar{v}}\right]$$

$\varepsilon_E^{\bar{v}} = \frac{\bar{v}}{q \cdot \bar{e}} \cdot \sum_{\mathrm{j}\in\mathrm{J}} \left[\frac{E_j}{v_j} \cdot \varepsilon_{E_j}^{v_j} \cdot \frac{\partial v_j}{\partial \bar{v}}\right]$ or:

$$\boldsymbol{\varepsilon_E^{\bar{v}} = \frac{\bar{v}}{\bar{e}} \cdot \sum_{\mathrm{j}\in\mathrm{J}} \left[\frac{f_j e_j}{v_j} \cdot \varepsilon_{E_j}^{v_j} \cdot \frac{\partial v_j}{\partial \bar{v}}\right].} \tag{27}$$

If we assume that speed changes proportionally for all vehicle classes, $\frac{\partial v_j}{\partial \bar{v}} = \frac{v_j}{\bar{v}}\ \forall\ \mathrm{j} \in \mathrm{J}$, then:

$$\boldsymbol{\varepsilon_E^{\bar{v}} = \frac{1}{\bar{e}} \cdot \sum_{\mathrm{j}\in\mathrm{J}} \left[e_j \cdot f_j \cdot \varepsilon_{E_j}^{v_j}\right] = \sum_{\mathrm{j}\in\mathrm{J}} \left[\frac{E_j}{E} \cdot \varepsilon_{E_j}^{v_j}\right].} \tag{28}$$

From this equation, emissions break-even conditions can also exist when decreased emissions from one vehicle class offset increased emissions from another, in addition to the general (trivial) case where $\varepsilon_{E_j}^{v_j} = 0\ \forall\ j \in J$.

Following previous emissions research (Sugawara and Niemeier, 2002; Barth and Boriboonsomsin, 2008), the functional form for $\bar{e} = f(\bar{v})$ employed in this paper is:

$$\boldsymbol{\bar{e}(\bar{v}) = \exp(\sum_{i=0}^{n}[a_i \cdot \bar{v}^i])\ ,} \tag{29}$$

where a_i are fitted parameters and $n = 4$. Similarly, class-average emissions rates, e_j, as a function of v_j are:

$$\boldsymbol{e_j(v_j) = \exp\left(\sum_{i=0}^{n}[a_{i,j} \cdot {v_j}^i]\right).} \tag{30}$$

The curves defined by equations **Error! Reference source not found.** and 30 are henceforth referred to as emissions-speed curves (ESC). By differentiating these ESC:

$$\boldsymbol{\varepsilon_{\bar{e}}^{\bar{v}} = \sum_{i=1}^{4}(i a_i \bar{v}^i)} \quad \textbf{and} \quad \boldsymbol{\varepsilon_{e_j}^{v_j} = \sum_{i=1}^{4}\left(i a_{i,j} v_j^{\,i}\right)}. \tag{31}$$

Note that $\varepsilon_{\bar{e}}^{\bar{v}}$, and $\gamma_{q}^{\bar{v}}$, are independent of q as long as $\bar{e} = f(\bar{v})$; the same independence from q holds for the class-specific variables.

ESC parameters a_i and $a_{i,j}$ are estimated using data points generated from the Motor Vehicle Emissions Simulator (MOVES) 2010 model from the U.S. Environmental Protection Agency (EPA, 2009a). The pollutants modeled are CO_2e (greenhouse gases in carbon-dioxide equivalent units), CO (carbon monoxide), NO_x (nitrogen oxides), $PM_{2.5}$ (particulate matter smaller than 2.5 microns), and HC (hydrocarbons). Emissions rates are modeled at 16 discrete average speeds (in 5-mph increments), and the parameters a_i and $a_{i,j}$ are estimated by minimizing squared error, with $\bar{e}$ and e_j in grams per vehicle mile and $\bar{v}$ and v_j in miles per hour. Note that $\bar{v}$ and v_j do not represent constant-speed driving, but are instead facility-specific average speeds representing archetypal driving-speed profiles.

The fitted ESC obtain $R^2 > 0.96$ for all five pollutants. Fitted parameters a_i and $a_{i,j}$ are shown in Table 7 for the full vehicle fleet and for light-duty (LD) and heavy-duty (HD) portions of the vehicle fleet on freeways for April 2010. The modeled full fleet is composed of 8.9% HD vehicles. Details of the MOVES model inputs and ESC fits are in Bigazzi (2011).

Table 7. MOVES Emissions-Speed Curve Fit Parameters for $\bar{e}$ and e_j

		CO_2e	CO	$PM_{2.5}$	NO_x	HC
Full Fleet	a_0	8.191	2.885	-1.223	1.897	0.3352
	a_1	-0.1826	-0.1788	-0.1769	-0.1656	-0.2040
	a_2	0.006339	0.006629	0.006640	0.005830	0.006643
	a_3	-9.690E-05	-1.092E-04	-1.127E-04	-8.928E-05	-1.012E-04
	a_4	5.357E-07	6.518E-07	6.724E-07	4.936E-07	5.674E-07
LD Vehicles	$a_{0,l}$	7.987	2.788	-2.856	0.3239	-0.2644
	$a_{1,l}$	-0.1856	-0.1760	-0.2000	-0.1152	-0.1878
	$a_{2,l}$	0.006352	0.006535	0.007365	0.004155	0.006173
	$a_{3,l}$	-9.550E-05	-1.077E-04	-1.157E-04	-6.270E-05	-9.570E-05
	$a_{4,l}$	5.210E-07	6.460E-07	6.560E-07	3.440E-07	5.510E-07
HD Vehicles	$a_{0,h}$	9.254	3.541	1.005	4.124	2.059
	$a_{1,h}$	-0.1748	-0.1900	-0.1740	-0.1839	-0.2206
	$a_{2,h}$	0.006307	0.006843	0.006599	0.006461	0.006967
	$a_{3,h}$	-1.007E-04	-1.097E-04	-1.141E-04	-1.003E-04	-1.018E-04
	$a_{4,h}$	5.740E-07	6.201E-07	6.870E-07	5.599E-07	5.380E-07

The next section applies these ESC parameters and the preceding equations to estimate the total emissions impacts of capacity-based congestion-mitigation strategies.

6.0 EMISSIONS IMPACTS OF CAPACITY-BASED CONGESTION MITIGATION (CBS)

The long-term net emissions effects of CBS can be estimated as $\varepsilon_E^{\bar{v}}$ from Equation **Error! Reference source not found.**, with modeled values for a_i and an expected value for travel-demand elasticity, $\eta_q^{\bar{v}}$ (which is highly uncertain). However, to estimate only the sign of net changes in emissions, it is only necessary to determine the value of the break-even demand elasticity $\gamma_q^{\bar{v}}$, which is dependent on average travel speed, vehicle-fleet composition, and ESC parameters. Three distinct scenarios are possible: (a) if $\eta_q^{\bar{v}} < \gamma_q^{\bar{v}}$ then CBS will likely decrease total emissions, (b) if $\eta_q^{\bar{v}} > \gamma_q^{\bar{v}}$ then CBS will likely *increase* total emissions, and (c) if $\eta_q^{\bar{v}} = \gamma_q^{\bar{v}}$ then total emissions are likely to be unaffected by changes in capacity and congestion in the long term.

The literature suggests that likely values of induced demand from capacity increases are in the range: $0.2 < \eta_q^{\bar{v}} < 1.0$ [1]. Using this range of likely elasticity values, Figure 7 shows qualitative characterizations of expected emissions effects of CBS for each pollutant over a range of speeds for the full modeled fleet on freeways – based on $\gamma_q^{\bar{v}} = -\sum_{i=1}^{4}\left(i a_i \bar{v}^i\right)$ and a_i from Table 7. As an emissions-reducing strategy, CBS are "not recommended" for $\gamma_q^{\bar{v}} < 0.25$; CBS are suggested to "apply with caution" for $0.25 \leq \gamma_q^{\bar{v}} < 0.5$; CBS have "potential benefits" for $0.5 \leq \gamma_q^{\bar{v}} < 0.75$; and CBS provide "good opportunity" for emissions reductions for $0.75 \leq \gamma_q^{\bar{v}}$. These are subjective, qualitative labels based on the demand-elasticity literature – see Bigazzi (2011) for an extensive discussion.

[1] The reader may wish to refer to meta-reviews on demand elasticity such as Goodwin et al., (2004) and Graham and Glaister (2004); also see Bigazzi (2011) for an extensive discussion.

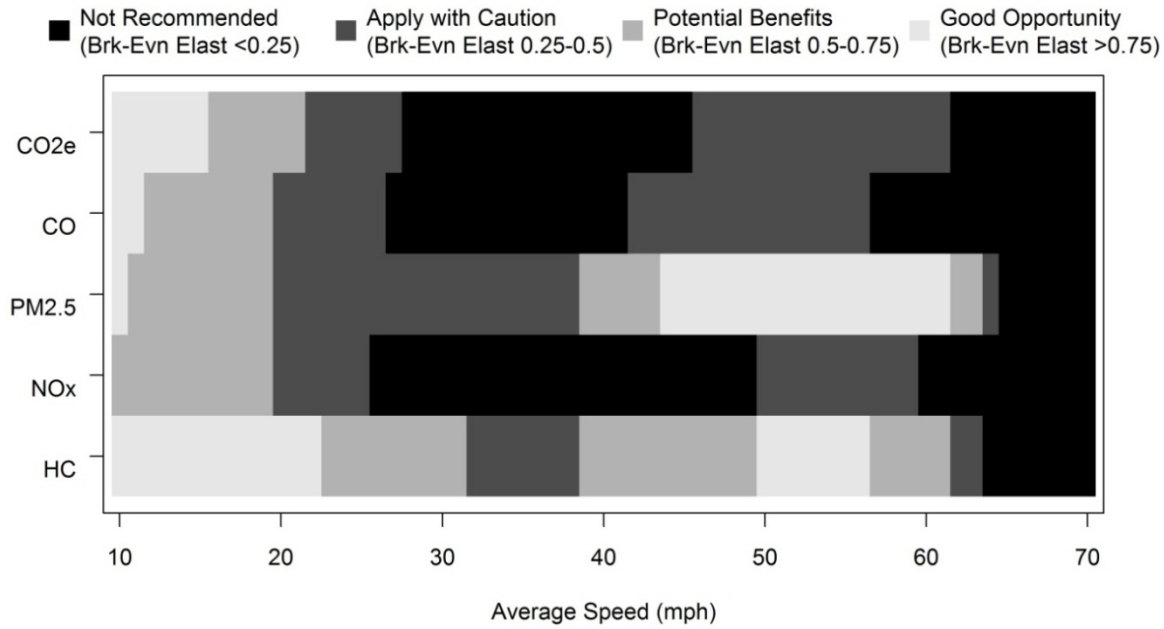

Figure 7. Characterization of CBS for emissions reductions

Beyond the potential subjectivity of the classification, it is evident from Figure 7 that CBS will have significantly different net impacts across pollutants. $PM_{2.5}$ and HC have the widest range of speeds for which CBS are likely to reduce total emissions. The other pollutants are only classified as "potential benefits" or better at speeds of about 20 mph and below. CBS are "not recommended" for all pollutants at speeds above 65 mph, showing the emissions benefits from limiting free-flow speeds to below 65 mph.

The characterizations in Figure 7 assume similar responses by vehicle type. Now consider a binary segmentation of the vehicle fleet where $j = l$ is all LD vehicles and $j = h$ is all HD vehicles: $J = \{l, h\}$. If we assume the extreme case of $\eta_{q_h}^{v_h} = 0$ (inelastic HD-vehicle travel demand to travel speed), then from Equation **Error! Reference source not found.**, $\varepsilon_E^{\bar{v}} = 0$ when $\eta_{q_l}^{v_l} = -\left(\frac{e_h \cdot f_h}{e_l \cdot f_l} \cdot \varepsilon_{e_h}^{v_h} + \varepsilon_{e_l}^{v_l}\right)$. Based on this net break-even demand elasticity for LD vehicles, Figure 8 shows a similar characterization of CBS to Figure 7, but assuming $\eta_{q_h}^{v_h} = 0$ (with initial $f_h = 0.09$ and $a_{i,j}$ from Table 7).

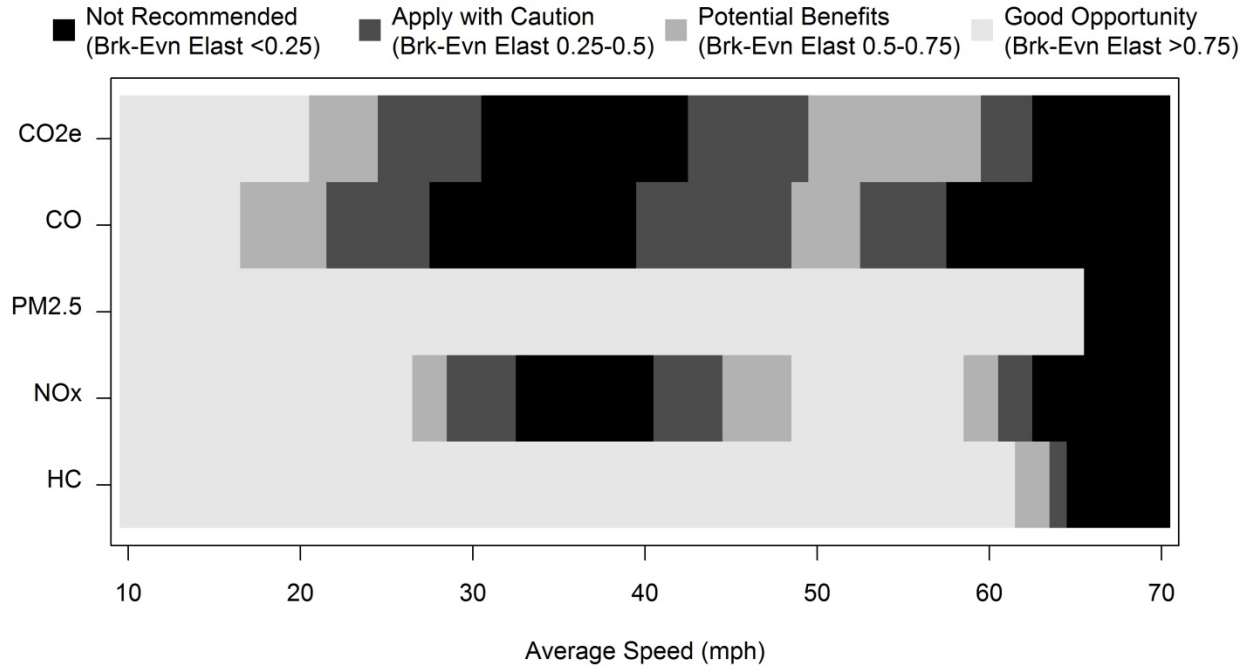

Figure 8. Characterization of CBS based on break-even demand elasticity for LD vehicles, assuming inelastic HD demand

The demand elasticity of HD vehicles is a major factor to determine net emissions changes. In Figure 8 there is a wider array of speeds for all pollutants that present opportunities for emissions reductions through CBS than in Figure 7. For $PM_{2.5}$ and HC, good opportunities exist for emissions reductions from CBS all the way up above 60 mph. Although this is perhaps an extreme value of demand elasticity for HD vehicles, it demonstrates that even at only 9% of the fleet, $\eta_{q_h}^{v_h}$ is an important consideration for predicting total emissions effects of congestion mitigation.

For this analysis to apply, CBS are not necessarily additional lane miles. Capacity or throughput can also be increased by various traffic-management strategies that target roadway efficiency and utilization, such as lane-change restrictions on freeways or effective management of variable speed limits. The key to the effects demonstrated here is an increase in average travel speed with baseline or higher traffic volumes.

Some traffic-management techniques could have implications for vehicle-speed profiles that would affect estimates of $a_{i,j}$ (we assumed $a_{i,j}$ parameters do not change in Figure 7 and Figure 8). For example, a significant "smoothing" of vehicle speeds could reduce the average emissions rate at a given average travel speed by reducing engine loads (Barth and Boriboonsomsin, 2008). This change in the ESC parameters would have to be considered in concert with any changes in average travel speed or travel-demand volume, but the same methodology can be applied to estimate long-term emissions impacts of CBS.

Similarly, emissions rates are expected to trend downward over time. If the *shape* of the ESC (i.e. $\varepsilon_{\bar{e}}^{\bar{v}}$) do not change, then the analysis is unaffected. If, on the other hand, advances in vehicle technology lead to vehicles that are less sensitive to congestion (i.e., flatter ESC), then the prospects of CBS are affected. This possibility is considered in the next section.

7.0 THE IMPACTS OF MORE EFFICIENT VEHICLES (EBS)

The results in Section 6.0 are for conventional internal combustion engine (ICE) vehicles only – the vast majority of the existing on-road fleet (U.S. Environmental Protection Agency, 2009b). We now examine the effects of introducing advanced vehicles in the fleet, a form of EBS. By reducing $\bar{e}$, EBS decrease total emissions as $\frac{\partial E}{\partial \bar{e}} = q$ (from Equation **Error! Reference source not found.**), and thus $\varepsilon_E^{\bar{e}} = 1$. But EBS can also impact the efficacy of CBS for emissions reductions. Let vehicle class $j = c$ be all conventional ICE vehicles, vehicle class $j = e$ be electric vehicles (EV), and vehicle class $j = a$ be other advanced efficiency (AE) vehicles. This is the complete set of vehicles, $J = \{c, a, e\}$, with total emissions of $E = E_c + E_a + E_e$. The total emissions elasticity to speed, from Equation 28, is then:

$$\boldsymbol{\varepsilon}_{\boldsymbol{E}}^{\bar{v}} = \frac{\boldsymbol{E_c}}{\boldsymbol{E}} \boldsymbol{\varepsilon}_{\boldsymbol{E_c}}^{\boldsymbol{v_c}} + \frac{\boldsymbol{E_a}}{\boldsymbol{E}} \boldsymbol{\varepsilon}_{\boldsymbol{E_a}}^{\boldsymbol{v_a}} + \frac{\boldsymbol{E_e}}{\boldsymbol{E}} \boldsymbol{\varepsilon}_{\boldsymbol{E_e}}^{\boldsymbol{v_e}} . \tag{32}$$

The AE vehicle class contains vehicles (such as many gas-electric hybrids) with regenerative braking and other improvements that render them less sensitive or insensitive to low-speed inefficiencies: i.e. $\left|\varepsilon_{e_a}^{v_a}\right| < \left|\varepsilon_{e_c}^{v_c}\right|$. Then, because $\varepsilon_{e_c}^{v_c}$ is expected to be negative through most of the range of feasible speeds according to the MOVES-based ESC, $\varepsilon_{e_c}^{v_c} < \varepsilon_{e_a}^{v_a} \leq 0$. Considering only emissions from ICE and AE vehicles ($E = E_c + E_a$), Equation **Error! Reference source not found.** reduces to:

$$\boldsymbol{\varepsilon}_{\boldsymbol{E}}^{\bar{v}} = \frac{\boldsymbol{E_c}}{\boldsymbol{E}} \boldsymbol{\varepsilon}_{\boldsymbol{E_c}}^{\boldsymbol{v_c}} + \frac{\boldsymbol{E_a}}{\boldsymbol{E}} \boldsymbol{\varepsilon}_{\boldsymbol{E_a}}^{\boldsymbol{v_a}} = \boldsymbol{\varepsilon}_{\boldsymbol{E_c}}^{\boldsymbol{v_c}} - \frac{\boldsymbol{E_a}}{\boldsymbol{E}} \left(\boldsymbol{\varepsilon}_{\boldsymbol{E_c}}^{\boldsymbol{v_c}} - \boldsymbol{\varepsilon}_{\boldsymbol{E_a}}^{\boldsymbol{v_c}} \right) . \tag{33}$$

If we assume that travel-demand elasticity is unaffected by vehicle type, $\eta_{q_j}^{v_j} = \eta_q^{\bar{v}} \; \forall \, j$, then using $\varepsilon_{E_j}^{v_j} = \eta_{q_j}^{v_j} + \varepsilon_{e_j}^{v_j}$, Equation **Error! Reference source not found.** further reduces to:

$$\boldsymbol{\varepsilon}_{\boldsymbol{E}}^{\bar{v}} = \boldsymbol{\varepsilon}_{\boldsymbol{E_c}}^{\boldsymbol{v_c}} - \frac{\boldsymbol{E_a}}{\boldsymbol{E}} \left(\boldsymbol{\varepsilon}_{\boldsymbol{e_c}}^{\boldsymbol{v_c}} - \boldsymbol{\varepsilon}_{\boldsymbol{e_a}}^{\boldsymbol{v_a}} \right) . \tag{34}$$

The value of $\varepsilon_{e_c}^{v_c} - \varepsilon_{e_a}^{v_a}$ is expected to be negative because it is assumed that $\varepsilon_{e_c}^{v_c} < \varepsilon_{e_a}^{v_a} \leq 0$. Thus, with an increase in E_a (because of higher f_a or $\boldsymbol{e_a}$), $\varepsilon_E^{\bar{v}}$ increases, too (becomes more positive or less negative). In other words, total emissions are more likely to increase with speed when there are more or higher-emitting AE vehicles in the fleet. The change can be explained by lower emissions-rate sensitivity to speed for AE vehicles: AE vehicles have less efficiency improvement than ICE vehicles with increasing speed, but still are subject to increased total emissions through induced demand.

From Equation **Error! Reference source not found.**, total emissions break-even conditions ($\varepsilon_E^{\bar{v}} = 0$) exist when:

$$\boldsymbol{\varepsilon_{E_c}^{v_c} = \frac{E_a}{E}\left(\varepsilon_{e_c}^{v_c} - \varepsilon_{e_a}^{v_a}\right)},$$

or substituting and combining terms:

$$\boldsymbol{\eta_q^{\bar{v}} = \frac{E_c}{E}\gamma_{q_c}^{v_c} + \frac{E_a}{E}\gamma_{q_a}^{v_a}}. \quad \textbf{(35)}$$

Because $\varepsilon_{e_c}^{v_c} < \varepsilon_{e_a}^{v_a} \leq 0$, we expect that $\gamma_{q_c}^{v_c} > \gamma_{q_a}^{v_a} \geq 0$, and thus the break-even demand elasticity with AE vehicles present is smaller than for ICE vehicles alone $\left(\gamma_{q_c}^{v_c}\right)$. In the extreme case, AE vehicles have emissions rates that are non-zero ($e_a \neq 0$), but that are insensitive to congestion level and average speed, $\varepsilon_{e_a}^{v_a} = \gamma_{q_a}^{v_a} = 0$. Then Equation **Error! Reference source not found.** reduces to $\eta_q^{\bar{v}} = \frac{E_c}{E}\gamma_{q_c}^{v_c}$ and the break-even demand elasticity is smaller in proportion to the fractional ICE emissions out of total emissions. Smaller values of break-even demand elasticity suggest *less* potential for emissions benefits from congestion mitigation. More AE vehicles are expected to decrease total emissions as they replace ICE vehicles, as long as $e_a < e_c$; but efficiency gains through speed increases are more likely to be cancelled out by induced demand, and CBS are less likely to be an effective emissions-reduction strategy with more AE vehicle emissions.

Regarding electric vehicles, if EV emissions are zero ($e_e = 0$ and by extension $\frac{\partial e_e}{\partial v_e} = \varepsilon_{e_c}^{v_c} = 0$), then equations **Error! Reference source not found.** and **Error! Reference source not found.** still apply. Unless a change in f_e affects the fraction of AE-vehicle emissions $\frac{E_a}{E}$ through a change in $\frac{f_a}{f_c}$**,** the total emissions elasticity to speed $\varepsilon_E^{\bar{v}}$ is independent of the fraction of EV in the fleet, f_e (even though EVs reduce emissions on a per-vehicle basis). Similarly, if the presence of EVs does not affect $\frac{f_a}{f_c}$, then the EVs will not impact break-even demand elasticity. If we choose to consider the upstream emissions for EV that are generated during the electric-power production process (i.e., using a "well-to-wheels" approach or life-cycle assessment (LCA)), then $0 < e_e < e_c$ and we can represent EV as a new type of AE vehicle – and the previous equations **Error! Reference source not found.** and **Error! Reference source not found.** are still applicable.

This section demonstrated the effects of EBS on the efficacy of CBS for emissions reductions. Section 6 will discuss the relative direct impacts of EBS as compared to CBS by analyzing three potential EBS, all of which reduce $\bar{e}$:

- Vehicle-fleet fuel-efficiency improvements (by lighter vehicles, less power-intensive engines, or a speed-smoothing "eco-driving" approach),

- Reduced fuel-carbon intensity (by using alternative fuels such as biodiesel or electricity, or by less energy-intensive fuel production and delivery methods), and
- Replacement of LD ICE vehicles in the fleet with LD EV.

But first we turn to a brief discussion of DBS for emissions reductions.

8.0 TRAVEL-VOLUME REDUCTIONS AND EMISSIONS (DBS)

Put simply in terms of the methodological framework, by reducing q, DBS decrease total emissions as $\frac{\partial E}{\partial q} = \bar{e}$ (from Equation **Error! Reference source not found.**), or $\varepsilon_E^q = 1$. But DBS also relate to congestion through the CBS analysis in Section 6.0.0. When $\eta_q^{\bar{v}} > \gamma_q^{\bar{v}}$, average speed-based efficiency alone cannot reduce total emissions because of induced travel demand. From the DBS perspective, when $\eta_q^{\bar{v}} > \gamma_q^{\bar{v}}$ a capacity *decrease* (i.e., "road diet") can reduce total emissions if the *suppressed* travel-demand volume offsets higher vehicle-emission rates at lower average travel speeds. In other words, with a capacity-based approach, lower total emissions are more likely by *increasing* capacity when $\eta_q^{\bar{v}} < \gamma_q^{\bar{v}}$ and by *decreasing* capacity when $\eta_q^{\bar{v}} > \gamma_q^{\bar{v}}$ [2].

In other forms of DBS vehicle-travel demand, volume is reduced by motivators such as road pricing or travel restrictions. For the demand-volume change alone, the emissions effect is indicated by $\varepsilon_E^q = 1$. If the DBS impacts congestion or is jointly implemented with a CBS, the key value for application of this analysis is the *net* travel-demand elasticity to travel speed. For example, if a demand-moderating measure such as road pricing is implemented along with a capacity expansion, then that effect can be incorporated as a lower expected range of $\eta_q^{\bar{v}}$. In the best case (for emissions), both increased average travel speeds and reduced travel-demand volume (i.e. $\eta_q^{\bar{v}} < 0$) contribute to a reduction of emissions (e.g., strong pricing programs such as implemented in London (Beevers and Carslaw, 2005)).

The next section describes the relative impacts of DBS as compared to CBS by assessing the emissions effects of reduced peak-period VMT per peak-period traveler (made possible by demand-management strategies).

[2] This assumes that demand elasticities to speed changes in each direction are the same (i.e., the aggregate travel response to a speed increase is equal and opposite of the response to a speed decrease).

9.0 COMPARING STRATEGIES FOR EMISSIONS REDUCTIONS

In this section we put emissions changes from CBS into context by comparison with a set of alternative EBS and DBS, with separate results for freeways and arterials. The analysis employs representative values for U.S. cities – with assumptions as described in Section 6.3.

9.1 FREEWAYS

We first look at freeways alone, comparing EBS and DBS to CBS that increase congested speeds as indicated by a level-of-service (LOS) change[3]. The comparison is presented as the amount of an EBS or DBS that would achieve equivalent emissions reductions to the CBS. Results for CO_2e emissions are shown in Table 8 using $\eta_q^{\bar{v}} = 0.3$ (a relatively low demand-elasticity value). The three numerical columns in Table 8 (from left to right) show LOS changes from F to E, from E to D, and from D to the A-C range. For each hypothetical LOS improvement, the net changes in average speed, travel-demand volume, and peak-period emissions are shown in the first three rows of the table. Only emissions from peak-period freeway travel are included, and the LOS changes only apply to the congested portion of freeway travel (55% – see assumptions in Section 6.3).

The final rows in Table 8 show the EBS and DBS changes that would be required to generate the same peak-period emissions changes on freeway facilities from each alternative strategy. The EBS and DBS effects apply to all peak-period freeway travel; other impacts are excluded (e.g., EV ownership would also reduce emissions from non-peak-period trips and from travel on non-freeway facilities).

[3] LOS is used as a qualitative congestion indicator, with average speeds for freeways from Barth et al. (1999). LOS F is the most congested, while LOS A through C are essentially at free-flow speeds.

Table 8. Equivalent Emissions Reduction Strategies for Freeway CO_2e ($\eta_q^{\bar{v}} = 0.3$)

	19 – 31 mph	31 – 53 mph	53 – 60 mph
Avg. speed change (mph)	11.9 (64%)	22.4 (73%)	6.8 (13%)
Travel demand change (vehicle miles/peak traveler-day)	0.7 (9%)	0.8 (10%)	0.2 (2%)
Net Emissions change (gCO_2e/peak traveler-day)	-131 (-3%)	112 (3%)	-31 (-1%)
Alternative Demand Strategy			
Trip length change (vehicle miles/peak traveler-day)	-0.2 (-3%)	0.2 (3%)	-0.1 (-1%)
Alternative Efficiency Strategies			
Vehicle efficiency change (miles/gallon)	0.5 (3%)	-0.5 (-3%)	0.2 (1%)
Fuel carbon intensity change ($kgCO_2e$/gallon)	-0.3 (-3%)	0.3 (3%)	-0.1 (-1%)
EV penetration by LCA (% of peak period fleet)	8%	-9%	3%
EV penetration by zero-emissions (% of peak period fleet)	4%	-4%	1%

As an example, consider the first numerical column of Table 8, which considers CO_2e emissions for a freeway LOS change from F to E. The average speed change on congested freeways from 19 to 31 mph (rounded) is a speed increase of 11.9 mph (64%) – row 1. Assuming $\eta_q^{\bar{v}} = 0.3$, this speed increase leads to 0.7 additional vehicle miles of peak-period freeway travel (per peak-period traveler per day), an increase of 9% – row 2. Considering the increased efficiency and induced demand, total CO_2e emissions are reduced by 131g per peak-period traveler, per day (-3%) – row 3. This 131g of emissions savings could also have been achieved by reducing daily peak-period freeway travel by 0.2 vehicle miles per peak-period traveler (-3%) – row 4. Alternatively, 131g of CO_2e could be saved if daily peak-period freeway travel were in vehicles with 0.5 miles per gallon higher fuel economy on average (3%) – row 5. A decrease of $0.3kgCO_2e$ per gallon (-3%) in the carbon intensity of fuel burned during peak-period freeway travel could also save 131g of CO_2e emissions – row 6. Finally, converting 8% (by LCA) or 4% (by zero-emissions estimation) of the LD-vehicle fleet to EV's for peak-period freeway travel could also achieve the same savings of 131g CO_2e – rows 7 and 8.

As expected from previous results, the LOS change from F to E generates the greatest emissions benefits in Table 8, which require the largest alternative strategies to match. These alternative strategies, subjectively modest but in some cases difficult to implement, have the potential for low- or zero-capital costs for transportation agencies (but lower fuel-tax revenue). On the other hand, capital improvement projects for CBS such as urban freeway widening can be extremely expensive endeavors (but they can increase fuel consumption and associated tax revenues).

At the moderate demand elasticity of $\eta_q^{\bar{v}} = 0.3$, the induced travel for LOS E to LOS D leads to a total emissions *increase*. When a total emissions increase is expected, the alternative strategy equivalents have opposite signs from an emissions savings (i.e., longer trips, reduced vehicle efficiency, higher fuel-carbon intensity, and fewer EVs in the fleet). Using an assumed elasticity of $\eta_q^{\bar{v}} = 0.5$, the induced travel leads to total emission increases for all three LOS improvements in Table 8.

9.2 ARTERIALS

Table 9 shows the results of an equivalent analysis for CO_2e emissions on arterials, again with a demand elasticity of $\eta_q^{\bar{v}} = 0.3$. Table 9 uses travel-speed increases of 10-16 mph, 16-24 mph, and 24-35 mph, roughly parallel to the heavily congested – moderately congested – uncongested LOS improvements in Table 8. As expected for a lower-speed facility, arterial congestion mitigation is more effective at reducing emissions rates. Still, even with this moderate demand elasticity the speed improvement above 24 mph produces a net emissions increase because of induced demand.

Table 9. Equivalent Emissions Reduction Strategies for Arterial CO_2e ($\eta_q^{\bar{v}} = 0.3$)

	10 – 16 mph	16 – 24 mph	24 – 35 mph
Avg. speed change (mph)	6.0 (60%)	8.0 (50%)	11.0 (46%)
Travel demand change (vehicle miles/peak traveler-day)	0.7 (9%)	0.6 (8%)	0.6 (7%)
Net Emissions change (gCO_2e/peak traveler-day)	-1,002 (-15%)	-374 (-7%)	31 (1%)
Alternative Demand Strategy			
Trips length change (vehicle miles/peak traveler-day)	-1.3 (-15%)	-0.6 (-7%)	0.1 (1%)
Alternative Efficiency Strategies			
Vehicle efficiency change (miles/gallon)	1.9 (17%)	1.1 (8%)	-0.1 (-1%)
Fuel carbon intensity change ($kgCO_2e$/gallon)	-1.3 (-15%)	-0.6 (-7%)	0.1 (1%)
EV penetration by LCA (% of peak period fleet)	29%	17%	-2%
EV penetration by zero-emissions (% of peak period fleet)	19%	9%	-1%

9.3 ASSUMPTIONS

The values in row 4 of tables 8 and 9 associated with VMT reductions (DBS) assume a fixed number of peak-period travelers and no change in average emissions rates (i.e., shorter or longer trips but the same and $\bar{v}$ and $\bar{e}$). The values in rows 5-8 (EBS) assume no changes in $\bar{v}$. Values in row 7 of tables 2 and 3 assume an EV carbon intensity of travel of 0.216 $kgCO_2e$ per mile (from the supplementary material of Samaras & Meisterling (2008)) based on LCA, although upstream emissions are not included in the on-road emissions estimates for ICE vehicles (a conservative approach). Tables 2 and 3, row 8, assume zero emissions for EVs; the assumption of zero emissions for EVs is also made for local pollutants in the results below.

Additional assumptions employed to calculate the figures contained in tables 2 and 3 include:

- Average daily peak-period travel on freeway and arterial facilities of 8.0 and 8.6 miles, respectively, per peak-period traveler (the average of 439 U.S. urban areas in 2007 –

extractable from the data tables accompanying the Urban Mobility Report (UMR) (Schrank and Lomax, 2009));

- Of peak-period freeway and arterial travel (by VMT), 55% is congested (the average of 439 U.S. urban areas in 2007 – again from the UMR data tables);
- Average fuel-carbon intensity measures 8.90 kgCO2e per gallon (calculated from (U.S. Environmental Protection Agency, 2009b));
- MOVES-based ESC parameters as shown in Table 7, with similar parameters for arterials from (Bigazzi, 2011);
- The portion of peak-period travel on uncongested freeways and arterials is assumed to have average speeds of 60 mph and 35 mph, respectively – emissions from travel on local roads is neglected (a conservative assumption for the EBS); and
- Induced demand is calculated using mid-point arc elasticity between two travel speed/travel volume conditions $(\bar{v}_1, VMT_1)$ and $(\bar{v}_2, VMT_2)$ as

$$\eta_q^{\bar{v}} = \frac{(VMT_2 - VMT_1)(\bar{v}_2 + \bar{v}_1)}{(VMT_2 + VMT_1)(\bar{v}_2 - \bar{v}_1)}. \quad \textbf{(1)}$$

9.4 FREEWAY/ARTERIAL COMPARISON

The net-percent emissions changes from CBS (row 3 of the preceding tables) for each facility-pollutant-LOS combination are shown in Figure 9, again using $\eta_q^{\bar{v}} = 0.3$ and the assumptions above. Positive values indicate emissions increases. Figure 9 shows that the largest emissions reductions from CBS are for heavily congested arterials. NO_x and CO emissions have almost no benefit from freeway congestion mitigation, while HC, the most speed-sensitive pollutant, has generally the highest potential savings.

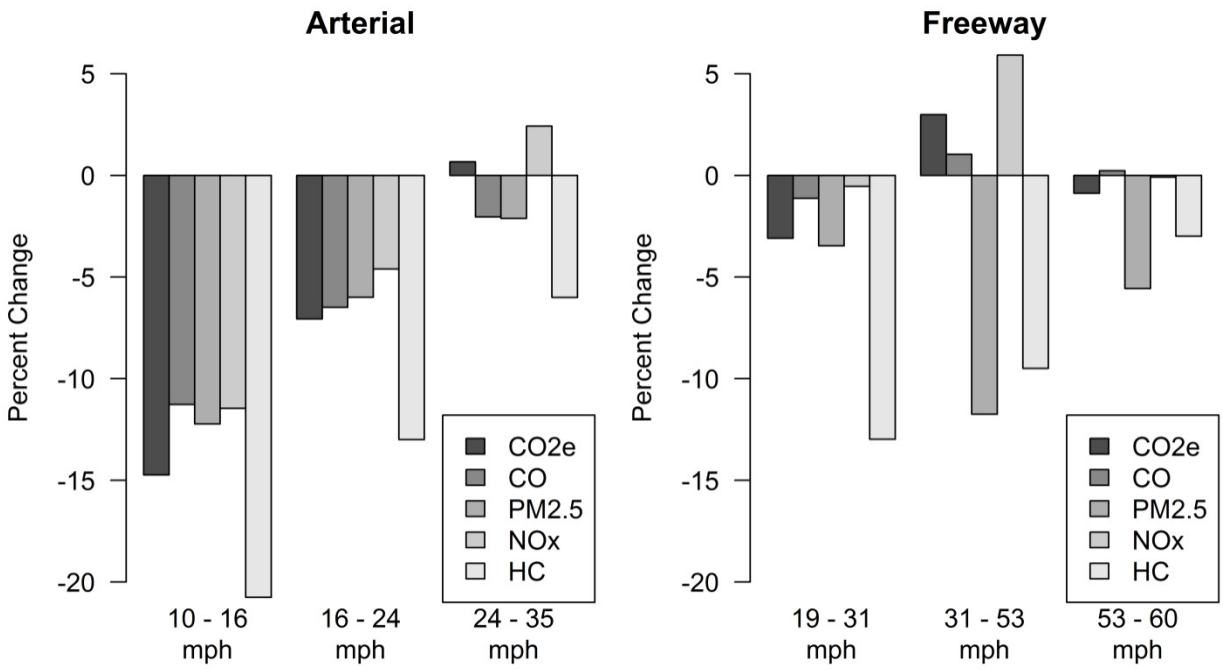

Figure 9: Percent change in peak-period emissions from CBS

9.5 EMISSIONS ELASTICITY TO EBS AND DBS

From the net emissions benefits of CBS shown in Figure 9, equivalent EBS and DBS are easily determined by their emissions elasticity. For VMT reductions (row 4, tables 2 and 3), increased fuel efficiency (row 5, tables 2 and 3), and decreased fuel-carbon intensity (row 6, tables 2 and 3) the total emissions point elasticity is -1. Thus, for these strategies a certain percentage emissions reduction from a CBS can also be accomplished by roughly the same percentage implementation of the EBS or DBS[4]. For example, the 3% reduction in CO_2e for the lowest-speed freeway improvement (Figure 9) can also be accomplished through a 3% reduction in VMT, a 3% increase in fuel efficiency, or a 3% decrease in fuel-carbon intensity.

For EV penetration of the fleet (rows 7 and 8 in tables 2 and 3) the emissions elasticity is slightly more complicated. Let $J = \{l, h, e\}$ where l and h are entirely ICE classes of LD and HD vehicles and e is a class of LD EV. If all EV are replacing LD ICE vehicles, then $\frac{\partial f_l}{\partial f_e} = -1$ and $\frac{\partial f_h}{\partial f_e} = 0$. The elasticity of E to f_e is then:

$$\boldsymbol{\varepsilon_E^{f_e} = \frac{1}{E}\frac{\partial E}{\partial f_e} = \frac{e_e - e_l}{\bar{e}}.} \quad \textbf{(37)}$$

If $e_e = 0$ (zero-emissions EV) and initially $f_e = 0$, then:

[4] The percent changes for vehicle efficiency in Table 2 and Table 9 are slightly different from the emissions savings because emissions are inversely related to efficiency, so the point elasticity of -1 will be different from the arc elasticity (which was used in the tables).

$$\boldsymbol{\varepsilon_E^{f_e} = \frac{-1}{1+f_h\left(\frac{e_h}{e_l}-1\right)}}. \quad \textbf{(38)}$$

The expected range of the ratio $\frac{e_h}{e_l}$ is from around 1 for CO up to 60 for $PM_{2.5}$ at low speeds (Bigazzi, 2011). Thus, using $f_h = 0.09$, $\varepsilon_E^{f_e}$ can range from -1.0 for CO to -0.16 for $PM_{2.5}$. Considering LCA EV emissions for CO_2e the elasticity is smaller: $\varepsilon_E^{f_e}$ changes by a factor of $\left(1 - \frac{e_e}{e_l}\right)$, or roughly 0.5 employing the assumptions previously described in this section. Since $-1 \leq \varepsilon_E^{f_e} < 0$, the total emissions elasticity to EV replacement of LD ICE vehicles is equal to or smaller than the emissions elasticity to the other EBS and DBS, and thus greater percent EV penetrations are needed.

Figure 10 shows the equivalent EV replacement results (i.e., rows 7 and 8 in tables 2 and 3) for all pollutants on both facilities, again assuming $\eta_q^{\bar{v}} = 0.3$. As expected, the percentages are larger than in Figure 9, in addition to having the opposite sign (because $-1 \leq \varepsilon_E^{f_e} < 0$). From the denominator of Equation **Error! Reference source not found.**, fleets with more HD vehicles (f_h) and pollutants with higher relative emissions rates from HD vehicles $\left(\frac{e_h}{e_l}\right)$ have smaller total emissions elasticity to EV penetration, $\varepsilon_E^{f_e}$. Smaller $\varepsilon_E^{f_e}$ means that EV replacement for LD vehicles is less effective at reducing total emissions. This effect is reflected in Figure 10, where $PM_{2.5}$ and NO_x (which have the highest $\frac{e_h}{e_l}$) are proportionally larger than the other pollutants when compared to Figure 9. The EV replacement of LD vehicles must be particularly large to reduce $PM_{2.5}$ because the $PM_{2.5}$ emissions are primarily from the HD portion of the vehicle fleet. Figure 10 shows that EBS that only reduce LD-vehicle emissions require large-scale deployment to be competitive with other strategies for reducing certain local pollutants.

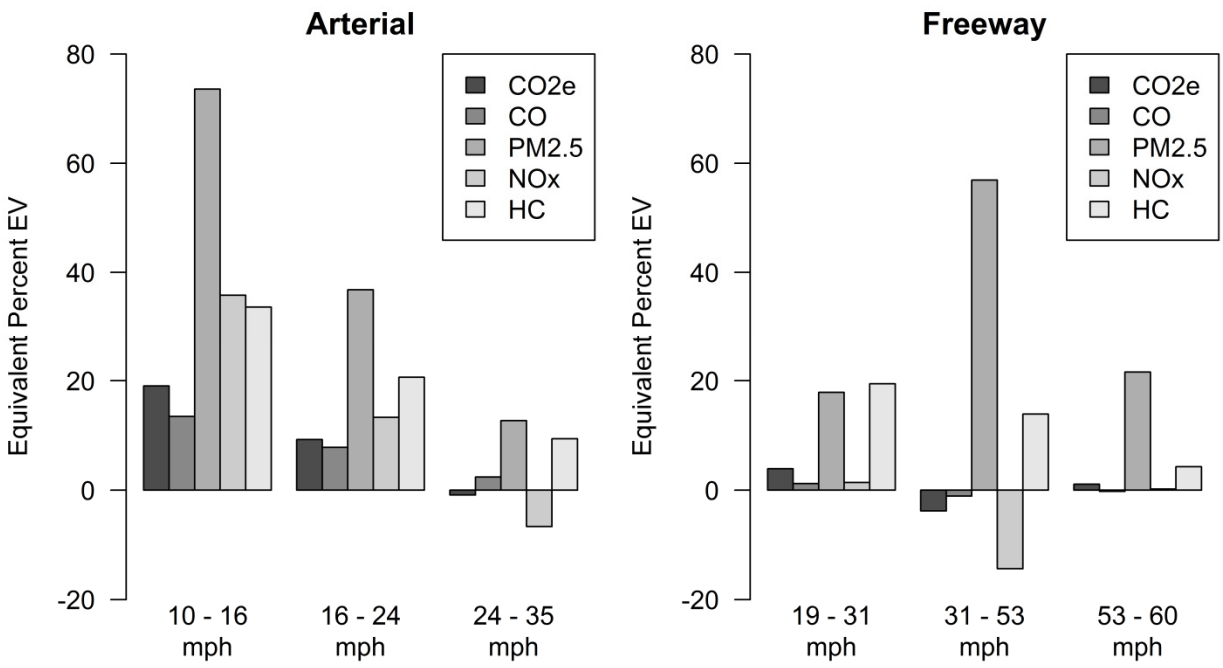

Figure 10. Zero-emissions LD EV penetration for equivalent EBS

10.0 CONSIDERATION OF VEHICLE CLASS-SPECIFIC STRATEGIES

The distinct emissions performance of LD and HD vehicles raises the potential for emissions co-benefits from more focused congestion-mitigation strategies that address vehicle classes separately. As a comparison of congestion- and emissions-mitigation approaches and their class-specific effects, Table 10 shows a short list of emissions-mitigation strategies with their expected direct impacts on the key variables of this analysis: travel speed v_j, travel volume q_j, emissions rate parameters $a_{i,j}$, and travel demand volume elasticity to speed $\eta_{q_j}^{v_j}$. The cells in the table are filled in with the relationships of an expected increase "+," decrease "–," or no change "o." These relationships are highly generalized, and actual impacts can depend on the details of implementation. Truck-only lanes (TOL) are roadway facilities that provide exclusive right-of-way for HD vehicles (Transportation Research Board, 2010). Just as general capacity expansions can employ road pricing to mitigate induced demand, TOL can utilize lane pricing (tolling) for the same purpose.

Table 10. Vehicle Class-Specific Congestion- and Emissions-Mitigation Strategy Impacts

	Light-Duty Vehicles				**Heavy-Duty Vehicles**			
Mitigation Strategy	v_l	q_l	$a_{i,l}$	$\eta_{q_l}^{v_l}$	v_h	q_h	$a_{i,h}$	$\eta_{q_h}^{v_h}$
General capacity increase	+	+	o	o	+	+	o	o
Truck-only lanes (no toll) – new capacity	+	+	o	o	+	+	o	o
Truck-only lanes (no toll) – appropriated capacity	–	–	o	o	+	+	o	o
Truck-only lanes (tolled) – new capacity	+	+	o	o	+	o	o	–
Truck-only lanes (tolled) – appropriated capacity	–	–	o	o	+	o	o	–
Congestion pricing/demand reduction strategies	+	–	o	–	+	–	o	–
Vehicle/fuel efficiency improvements	o	o[1]	–	o	o	o [1]	–	o

[1] Assuming fuel cost savings do not lead to induced travel

Capacity expansions (CBS) increase v_j and q_j, and the total emissions effect depends on the relative magnitude of each, as demonstrated earlier in this paper. The impacts of TOL on LD vehicles depend on whether (a) the TOL are added capacity (in which case v_l and q_l would both likely increase with the relocation of HD vehicles), or (b) the TOL are appropriated general-purpose capacity (in which case the capacity decrease for LD vehicles would likely lower v_l and q_l, though traffic-flow impacts of this type of TOL vary (Transportation Research Board, 2010)). A tolled TOL can have similar efficiency benefits without an increase in q_h by offsetting the travel-time savings with toll costs (reducing the effective value of $\eta_{q_h}^{v_h}$).

Congestion pricing and other forms of DBS reduce effective demand elasticity to travel speed, $\eta_{q_j}^{v_j}$ – but can also increase v_j by decreasing q_j and so reduce e_j. EBS include improvements in vehicle and fuel efficiency that reduce e_j by reducing the ESC parameters $a_{i,j}$, with the only likely impact on q_j or v_j being possible induced demand through a rebound effect due to decreased travel costs. The net effect of any of the strategies in Table 10 on total emissions can be determined by the joint evaluation of $\varepsilon_{e_j}^{v_j}$ and $\eta_{q_j}^{v_j}$, representing tradeoffs between vehicle efficiency and volume. The analytical framework presented in this paper allows for a parsimonious sketch-level analysis and comparison of various congestion and emissions-mitigation strategies.

11.0 CONGESTION-MITIGATION STRATEGIES CONCLUSIONS

This research is a step toward better understanding the potential emissions co-benefits of congestion-mitigation strategies. A novel methodological framework is applied to assess the total emissions effects of capacity-, demand- and efficiency-based emissions-reduction strategies. The net change in emissions depends on the balance of induced travel demand and increased vehicle efficiency – which, in turn, depend on the pollutant of interest, existing congestion level, and vehicle-fleet composition. Several interesting results are found by employing aggregate data representing average U.S. congestion and vehicle-fleet conditions.

Congestion mitigation does not inevitably lead to reduced emissions. Furthermore, the net effect of congestion mitigation will greatly depend on the type of emissions being analyzed. In general, capacity-based congestion reductions within certain speed intervals (e.g., 30 to 40 mph) can be expected to increase total emissions of CO_2e, CO, and NO_x in the long run through increased vehicle-travel volume. Wider speed ranges will see increased total emissions in more specific conditions. Vehicle emissions of HC and $PM_{2.5}$ have greater potential for reductions through traffic-congestion mitigation than CO_2e, CO or NO_x.

Fleet composition and vehicle class-relative emissions rates are also key factors to understand future impacts of congestion- and emissions-mitigation strategies. Reducing light-duty vehicle emissions alone has only a small impact on total $PM_{2.5}$ emissions – and a limited impact on other pollutants as well. Emissions-reduction strategies must also seek efficiency improvements for heavy-duty vehicles. Furthermore, even as a small fraction of the vehicle fleet, the demand elasticity of heavy-duty vehicles is important for predicting the total emissions effects of general congestion mitigation. Advanced-efficiency vehicles with emissions rates that are less sensitive to congestion than conventional vehicles generate less emissions co-benefits from congestion-mitigation strategies.

Applying hypothetical level-of-service (LOS) improvements reveals that large speed increases (percentage-wise) lead to comparatively small or non-existent net reductions in emissions. The largest potential emissions reductions for all pollutants are on heavily congested arterials; on freeways, large potential reductions are only seen for HC and $PM_{2.5}$ emissions. Comparing these capacity-based mitigation strategies with alternative approaches shows that the same or more emissions benefits can be achieved by demand- or efficiency-based emissions-reduction strategies. However, this research does not include all the complex tradeoffs among emissions, transportation-system performance, livability, capital investment and budget, and fuel-tax revenues.

The results presented in this paper are clearly dependent on the input data assumptions. This analysis uses aggregate data for current U.S. conditions, but the same methodological framework could be applied at any location where different values or strategies are expected. For example,

Section 0 describes how this methodological framework would apply for comparing vehicle class-specific congestion-mitigation strategies such as truck-only lanes.

REFERENCES

Barth, Matthew, and Kanok Boriboonsomsin. 2008. Real-World Carbon Dioxide Impacts of Traffic Congestion. Transportation Research Record: Journal of the Transportation Research Board 2058: 163–171.

Barth, M., Scora, G., Younglove, T., 1999. Estimating emissions and fuel consumption for different levels of freeway congestion. Transportation Research Record: Journal of the Transportation Research Board 1664, 47–57.

Beevers, S.D., Carslaw, D.C., 2005. The impact of congestion charging on vehicle emissions in London. Atmospheric Environment 39, 1–5.

Bigazzi, A., 2011. Traffic Congestion Mitigation as an Emissions Reduction Strategy (Thesis in Support of a Master of Science Degree in Civil and Environmental Engineering). Portland State University, Portland, Oregon.

Bigazzi, Alexander, and Miguel Figliozzi. 2011. An Analysis of the Relative Efficiency of Freeway Congestion Mitigation as an Emissions Reduction Strategy. Proceedings of the 90th Annual Meeting of the Transportation Research Board. Washington, D.C., January 25.

Boyles, Stephen D., Kara M. Kockelman, and S. Travis Waller. 2010. Congestion pricing under operational, supply-side uncertainty. Transportation Research Part C: Emerging Technologies 18, no. 4 (August): 519-535.

Brilon, W., J. Geistefeldt, and M. Regler. 2005. Reliability of freeway traffic flow: a stochastic concept of capacity. In Transportation and traffic theory: flow, dynamics and human interaction: proceedings of the 16th International Symposium on Transportation and Traffic Theory, University of Maryland, College Park, Maryland, 19-21 July 2005, 125.

Brownstone, David, and Kenneth A. Small. 2005. Valuing time and reliability: assessing the evidence from road pricing demonstrations. Transportation Research Part A: Policy and Practice 39, no. 4 (May): 279-293.

Bureau of Public Roads. 1964. Traffic Assignment Manual. U.S. Department of Commerce.

Castillo, J. M. Del, and F. G. Benítez. 1995. On the functional form of the speed-density relationship--I: General theory. Transportation Research Part B: Methodological 29, no. 5 (October): 373-389.

Chen, Anthony, Hai Yang, Hong K. Lo, and Wilson H. Tang. 2002. Capacity reliability of a road network: an assessment methodology and numerical results. Transportation Research Part B: Methodological 36, no. 3 (March): 225-252.

Danielis, Romeo, Edoardo Marcucci, and Lucia Rotaris. 2005. Logistics managers' stated preferences for freight service attributes. Transportation Research Part E: Logistics and Transportation Review 41, no. 3 (May): 201-215.

Dowling, R.G., 2005. Predicting air quality effects of traffic-flow improvements: final report and user's guide (NCHRP No. 535). Transportation Research Board.

European Conference of Ministers of Transport (ECMT). 2007. Managing Urban Traffic Congestion. OECD, Transport Research Center.

Federal Highway Administration, 2010. Congestion Mitigation and Air Quality (CMAQ) Improvement Program [WWW Document]. URL http://www.fhwa.dot.gov/environment/cmaqpgs/

Goodwin, P. 2004. The economic costs of road traffic congestion. Discussion Paper. London, UK: The Rail Freight Group.

Graham, D.J., Glaister, S., 2004. Road traffic demand elasticity estimates: a review. Transport Reviews 24, 261–274.

Grant, M., Kuzmyak, R., Shoup, L., Hsu, E., Krolik, T., Ernst, D., 2008. SAFETEA-LU 1808: CMAQ Evaluation and Assessment, Phase I Final Report (No. FHWA-HEP-08-019). Federal Highway Administration, Washington, D.C.

HDR. 2009. Assessing the Full Costs of Congestion on Surface Transportation Systems and Reducing Them through Pricing. U.S. DOT, February.

Figliozzi, Miguel and Meead Saberi, 2011. A Study of Freeway Stochastic Capacity and Travel Time Approximations Using Archived Loop Detector Data. Working Paper. Portland State University.

Kerner, B. S. 1999. Congested traffic flow: Observations and theory. Transportation Research Record: Journal of the Transportation Research Board 1678, no. 1: 160–167.

Kriger, David, Cristobal Miller, Mark Baker, and Fannie Joubert. 2007. Costs of Urban Congestion in Canada: A Model-Based Approach. Transportation Research Record: Journal of the Transportation Research Board 1994 (January 1): 94-100.

Lam, William H.K., Hu Shao, and Agachai Sumalee. 2008. Modeling impacts of adverse weather conditions on a road network with uncertainties in demand and supply. Transportation Research Part B: Methodological 42, no. 10 (December): 890-910.

Lo, Hong K., X.W. Luo, and Barbara W.Y. Siu. 2006. Degradable transport network: Travel time budget of travelers with heterogeneous risk aversion. Transportation Research Part B: Methodological 40, no. 9 (November): 792-806.

Lo, Hong K., and Yeou-Koung Tung. 2003. Network with degradable links: capacity analysis and design. Transportation Research Part B: Methodological 37, no. 4 (May): 345-363.

Lu, X. Y, and A. Skabardonis. 2007. Freeway Traffic Shockwave Analysis: Exploring the NGSIM Trajectory Data. Proceedings of the 86th Annual Meeting of the Transportation Research Board, Washington, DC.

May. 1989. Traffic Flow Fundamentals. Facsimile. Prentice Hall, December 17.

Noland, R.B., Quddus, M.A., 2006. Flow improvements and vehicle emissions: Effects of trip generation and emission control technology. Transportation Research Part D 11, 1–14.

Olson, P. L., D. E. Cleveland, P. S. Fancher, L. P. Kostyniuk, and L. W. Schneider. 1984. NCHRP Report 270: Parameters Affecting Stopping Sight Distance. Washington D.C.: Transportation Research Board, National Research Council.

Samaras, C., Meisterling, K., 2008. Life Cycle Assessment of Greenhouse Gas Emissions from Plug-in Hybrid Vehicles: Implications for Policy. Environmental Science & Technology 42, 3170–3176.

Schrank, David, and Tim Lomax. 2009. The 2009 Urban Mobility Report. College Station, TX: Texas Transportation Institute, July.

Stathopoulos, F.G., Noland, R.B., 2003. Induced travel and emissions from traffic flow improvement projects. Transportation Research Record: Journal of the Transportation Research Board 1842, 57–63.

Sugawara, S., Niemeier, D., 2002. How much can vehicle emissions be reduced? Exploratory analysis of an upper boundary using an emissions-optimized trip assignment. Transportation Research Record: Journal of the Transportation Research Board 1815, 29–37.

Transportation Research Board, 2002. The Congestion Mitigation and Air Quality Improvement Program: Assessing 10 Years of Experience (Special Report No. 264). National Academies, Washington, D.C.

Transportation Research Board, 2010. Separation of Vehicles - CMV-Only Lanes (NCHRP No. 649). National Academies, Washington, D.C.

U.S. Department of Transportation. n.d. ITS Benefits Database.

U.S. Environmental Protection Agency. 2009a. Light-Duty Automotive Technology, Carbon Dioxide Emissions, and Fuel Economy Trends: 1975 Through 2009. Washington, D.C.: U.S. Environmental Protection Agency, November.

U.S. Environmental Protection Agency 2009b. Motor Vehicle Emission Simulator (MOVES) 2010 User's Guide. Washington, D.C.: U.S. Environmental Protection Agency, December.

U.S. Environmental Protection Agency, 2009c. Light-Duty Automotive Technology, Carbon Dioxide Emissions, and Fuel Economy Trends: 1975 Through 2009 (No. EPA420-S-09-001). Washington, D.C

Weisbrod, G., D. Vary, and G. Treyz. 2001. NCHRP Report 463: Economic Implications of Congestion. Washington, D.C.: Transportation Research Board.

Zhang, Lei, and David Levinson. 2004. Some Properties of Flows at Freeway Bottlenecks. Transportation Research Record: Journal of the Transportation Research Board 1883, no. 1: 122-131.

P.O. Box 751
Portland, OR 97207

OTREC is dedicated to stimulating and conducting collaborative multi-disciplinary research on multi-modal surface transportation issues, educating a diverse array of current practitioners and future leaders in the transportation field, and encouraging implementation of relevant research results.